A Mathematical Understanding of Red Blood Cell Dynamics

By

Benjamin Brindle

Senior Honors Thesis

Advised by
Dr. Miranda I. Teboh-Ewungkem, Lehigh University
(Professor of Practice in Mathematics)

Department of Mathematics
Lehigh University
Bethlehem, Pennsylvania, United States
May 2021

Acknowledgements

I would first like to thank my research advisor, Dr. Miranda Teboh-Ewungkem, for her continued support during this my work on this thesis. Due to her guidance, I have developed into an independent researcher. I also thank the Lehigh University Math Department for allowing me to undertake this work and providing support for me to attend and present at numerous conferences during the development of this thesis.

Although the work done in this thesis deviates from the epidemiological work under the NSF Grant DMS-1814659, my undergraduate research related to this subject commenced via the support of this NSF grant. While independent from this thesis, my undergraduate research under NSF Grant DMS-1814659 enabled me to form a path to undertake this thesis. I would like to thank the NSF for this opportunity, as well as Dr. Carrie Manore (Los Alamos National Laboratory) and Dr. Douglas J. Perkins (University of New Mexico), who were collaborators under this grant and provided invaluable encouragement and support before my work on this thesis began. My collaboration with colleagues at Los Alamos National Laboratory was instrumental in encouraging my pursuit of research, and I thank Dr. Teboh-Ewungkem for facilitating these interactions.

Abstract

Red blood cells are one of the most important components of life in humans and other mammals. Loss of red blood cells has consequences, such as anemia, while overproduction of red blood cells can also have negative consequences. Losses can be the result of phlebotomy, parasitemia, or other diseases, and overproduction can be due to myeloproliferative disorders such as Polycythemia Vera. Red blood cell dynamics within a human involve several stages of precursor cells before a red blood cell fully matures to an erythrocyte. Upon perturbation, a feedback mechanism contingent on loss and level of erythrocytes causes the production of more precursor cells to attempt to return the blood dynamics to equilibrium. We model this process using a system of nonlinear, deterministic, ordinary differential equations. Functions describing this feedback, the stem cell recruitment, and the erythrocyte loss are chosen to examine the system dynamics in different scenarios. Some parameter choices cause a Hopf bifurcation, demonstrating the sensitivity of blood dynamics to the selected parameters. Numerical methods are used to display bifurcation diagrams and transient dynamics for specific function choices. Methods of mathematical analysis such as nondimensionalization and proofs of invariance, positivity, boundedness, and uniqueness for arbitrary functions are given.

Chapter 1

Introduction and Background

Red blood cells are one of the most important components of life in humans and other mammals. Red blood cells are produced through erythropoiesis [8], a component process of hematopoiesis, which develops erythropoietic stem cells into mature red blood cells (erythrocytes). In many adult mammals, such as humans, these stem cells are exclusively produced in the bone marrow, while in others, such as mice, they are additionally produced in the spleen, especially ewhen there is an increased demand for red blood cells [5]. Erythropoiesis involves several stages of precursors as cells develop from stem cells to erythrocytes. Early stages are sensitive to erythropoietin (EPO), while more mature stages are insensitive to EPO. EPO acts as a feedback mechanism regulating erythropoiesis by meeting the oxygen demand of tissues and controlling the production of precursors so that, in a healthy mammal, the production of red blood cells will be equal to the natural death of red blood cells through apoptosis. The study of red blood cell dynamics is important due to the number of health-related problems associated with red blood cells. For example, malaria parasitemia can cause blood loss, leading to anemia, while myeloproliferative disorders such as Polycythemia Vera can cause an overproduction of blood cells so extreme that phlebotomy may be necessary to mitigate the effects of the disease. Furthermore, red blood cell dynamics are not only relevant to the study of disease, but also the menstrual cycle, where blood loss must be regulated to ensure females are not anemic.

Red blood cell dynamics present a scenario that can be studied mathematically to depict the relevant dynamical processes using functional responses. Mackey [9] provided one of the earliest [15] mathematical approaches to modelling aplastic anemia and its origin in hematopoietic stem cells. In contrast to myeloproliferative disorders, aplastic anemia causes insufficient production of blood cells. Together with Glass [10], Mackey helped establish the legitimacy of mathematical modeling as a tool to study dynamical blood diseases. Later work, particularly that of Fuertinger et al. [4] and Tetschke et al. [17], examine erythropoiesis in more detail in specific settings. Fuertinger et al. mathematically explore the situations of recovery after blood donation and adjustment to altitude change, while Tetschke et al. concentrates on a general erythropoiesis model's application to Polycythemia Vera. Thibodeaux [18] and Fonseca and Voit [3] provide mathematical models of erythropoiesis under malaria infection. The former showed that the number of parasites produced during the destruction of each erythrocyte has the most significant impact on erythropoiesis and the removal of the toxin hemozoin, used by the parasite to suppress erythropoiesis, may speed recovery of the erythrocyte population. The latter compared several frameworks to model erythropoiesis subject to malaria, finding that discrete recursive equations best captured the dynamics at play. The works mentioned above provide only a sample of the number of red blood cell diseases and situations that can be mathematically modeled to elucidate their underlying dynamics. As such, the development of a generalized mathematical model that can be applied to consider both different external loss factors and different internal factors of blood cell production for numerous situations has clear benefits, as previous work in this field can be examined through the lens of a single model.

The application of this model to studying malaria parasitemia is particularly important. According to the 2020 World Malaria Report [14], there were approximately 409,000 malaria deaths in 2019, with 67% of which were among children aged under 5 years. Mathematically, the interaction of the malaria parasite within the blood is equivalent in form to a predator-prey interaction where the parasite attacks and infects healthy red blood cells. Like in conventional predator-prey models, the survival of the malarial parasite is contingent upon the continued existence of red blood cell prey. A mathematical model examining the dynamics of blood loss under malaria could help guide medical decisions surrounding the detection of malarial anemia.

In this work, we present a generalized mathematical model of erythropoiesis during loss. This model allows for the implementation of different functional choices to model production of erythrocytes, regulatory feedback, and blood loss due to external factors. This model can be applied to several scenarios with appropriate functional choices, such as Polycythemia Vera, malaria, and loss due to menstruation. Utilization of both mathematical and numerical tools help to illustrate the red blood cell dynamics of these situations.

1.1 Definitions

1.1.1 Biological Definitions

- Anemia: A condition in which the body lacks red blood cells.
- Aplastic anemia: A condition in which the body does not produce enough red blood cells to maintain healthy levels.
- EPO: Erythropoietin, a hormone produced primarily by the kidneys which plays a key role in the production of red blood cells by stimulating the production of BFU-E cells, CFU-E cells, and some erthryoblasts to respond to the oxygen demand of tissues.
- Erythrocytes: Synonymous with mature red blood cells.

- Erythropoiesis: The process of forming mature erythrocytes (a part of hematopoiesis).
- Hematopoiesis: The process of forming blood cells.
- Malaria: A disease caused by infection by a parasite transmitted by the bite of infected mosquitoes. The merozoite stage of the malaria parasite grows within infected red blood cells, ultimately causing the demise of the cell as it bursts to release more parasites into the blood.
- Myeloproliferative disorders: Disorders which can stimulate the production of red blood cells, white blood cells, and platelets.
- Neocytolysis: A physiologic process in which immature erythrocytes are selectively destroyed.
- Phlebotomy: Synonymous with bloodletting.
- Polycythemia vera: The most common myeloproliferative disorder, it causes an increase in red blood cell production.
- Red blood cells: The most common blood cell in vertebrates and the primary means of transporting oxygen to body tissues.
- Reticulocytes: Immature red blood cells without a nucleus
- Stem cell: Cells that can develop into specialized cell types within the body.

1.1.2 Mathematical Definitions, Terminologies, and Preliminary Material

Definition 1. *An **ordinary differential equation** is an equation involving ordinary derivatives in one variables of an unknown, independent variable, rather than partial derivatives. [1]*

Theorem 1. ***Existence and Uniqueness Theorem**: For the nth-order system $\dot{\mathbf{x}} = \mathbf{f}(\mathbf{x}, t)$, suppose that $\mathbf{f}$ is continuous and that $\partial f_j/\partial x_i$, i, $j = 1, 2, \ldots, n$ are continuous for $x \in \mathcal{D}$, $t \in \mathbf{I}$, where $\mathcal{D}$ is a domain and $\mathbf{I}$ is an open interval. Then if $x_0 \in \mathcal{D}$ and $t_0 \in \mathbf{I}$, there exists a solution $\mathbf{x}^*(t)$, defined uniquely in some neighbourhood of $(\mathbf{x_0}, t_0)$, which satisfies $\mathbf{x}^*(t_0) = \mathbf{x_0}$. [7]*

Definition 2. *A solution to a system of ordinary differential equations $\dot{\mathbf{x}} = \mathbf{f}(\mathbf{x}, t)$ with initial condition $\mathbf{x}(t_0) = \mathbf{x_0}$ is **unique** if there exists only one solution $\mathbf{x}^*$ solving the system with the given conditions. [2]*

Definition 3. *A solution to a system of ordinary differential equations $\dot{\mathbf{x}} = \mathbf{f}(\mathbf{x}, t)$ with initial condition $\mathbf{x}(t_0) = \mathbf{x_0}$ is **bounded above** if there exists some constant, finite vector $\mathbf{U}$ such that $\mathbf{x}(t) < \mathbf{U}$ for all t. Similarly, the same solution is **bounded below** if there exists some constant, finite vector $\mathbf{L}$ such that $\mathbf{L} < \mathbf{x}(t)$ for all t. [2]*

Definition 4. *A system of ordinary differential equations* $\dot{\mathbf{x}} = \mathbf{f}(\mathbf{x}, t)$ *with initial condition* $\mathbf{x}(t_0) = \mathbf{x_0}$ *is* ***positively invariant*** *if, for a solution* $\mathbf{x}(t)$ *of the problem,* $\mathbf{x}(0) \in \mathbb{R}^n_+$ *(vectors in* $\mathbb{R}^n$ *with strictly positive components) implies that* $\mathbf{x}(t) \in \mathbb{R}^n_+$ *for all* $t > 0$*. [7]*

Definition 5. *A* ***steady state*** *or* ***equilibrium point*** *of a system of ordinary differential equations* $\dot{\mathbf{x}} = \mathbf{f}(\mathbf{x}, t)$ *with initial condition* $\mathbf{x}(t_0) = \mathbf{x_0}$ *is a point* $(\mathbf{x_s}, t_s)$ *at which* $f(\mathbf{x_s}, t_s) = 0$*. [7]*

Terminology 1. ***Nondimensionalization*** *is the removal of physical dimensions from an equation or system by a substitution of variables.*

Definition 6. *The* ***Jacobian matrix*** J *of a system of* n *ordinary differential equations* $\dot{\mathbf{x}} = \mathbf{f}(\mathbf{x}) = [f_1(\mathbf{x}), \ldots, f_n(\mathbf{x})]^T$ *evaluated at the equilibrium point* $\mathbf{x} = \mathbf{x_c}$ *is the* $n \times n$ *matrix with elements given by* $J_{ij} = [\frac{\partial f_i(\mathbf{x})}{\partial x_j}]_{\mathbf{x}=\mathbf{x_c}}$*. [7]*

Definition 7. *The* ***characteristic polynomial*** $p_A(\lambda)$ *of an* $n \times n$ *matrix* A *is a monic polynomial of degree* n *defined by* $p_A(\lambda) = \det(A - \lambda I)$*, where* I *is the* $n \times n$ *identity matrix. The eigenvalues of* A *are the roots of* $p_A(\lambda)$*. [7]*

Terminology 2. *The* ***stability*** *of an equilibrium point of a system of ordinary differential equations is determined by the behavior the solution following a perturbation away from equilibrium. The stability of an equilibrium point can be classified from the eigenvalues of the Jacobian matrix of the system evaluated at that equilibrium point. For instance, a stable equilibrium corresponds to a Jacobian matrix that has eigenvalues with all negative real parts. [1]*

Definition 8. *A* ***bifurcation*** *of a system of ordinary differential equations occurs at a point where a small change to parameter values of the system causes a sudden qualitative change in solution behavior. Local bifurcations change stability properties of equilibrium points. A* ***Hopf bifurcation*** *occurs at an equilibrium point* $\mathbf{x_h}$ *when a change in parameter values causes an eigenvalue of the Jacobian matrix corresponding to* $\mathbf{x_h}$ *to have zero real part with nonzero imaginary part. [7]*

Statement 1. ***Descartes' rule of signs*** *states that the number of positive real roots of a polynomial* $p(x) = a_n x^n + a_{n-1} x^{n-1} + \cdots + a_1 x + a_0$ *is at most the number of sign changes in the sequence* $\{a_i : a_i \neq 0\}$ *of nonzero coefficients of* $p(x)$*. The difference between the actual number of positive real roots of* $p(x)$ *and the number of sign changes of the nonzero coefficients is always an even number. If the number of sign changes is one, there will be one positive real root. Similarly, if there are no sign changes, there will be no positive real roots.*

Definition 9. *A system of differential equations* $\dot{\mathbf{x}} = \mathbf{f}(\mathbf{x})$ *is a* ***monotone system*** *if* $\mathbf{x} \leq \mathbf{y}$ *implies* $\phi_t(\mathbf{x}) \leq \phi_t(\mathbf{y})$ *for any* $t \geq 0$*, where* $\phi_t(x)$ *is the trajectory at* t *started from* $\mathbf{x}$*. [16]*

Definition 10. *A function* $x \mapsto f(x)$ *is* ***Lipschitz continuous*** *if there exists a positive real number* L *such that* $||f(x) - f(y)|| \leq L||x - y||$ *for all* x *and* y *in the domain. [2]*

Statement 2. *The* ***Routh-Hurwitz Criterion*** *for a* ***degree 3 monic polynomial*** $p(\lambda) = \lambda^3 + a_1\lambda^2 + a_2\lambda + a_3$ *states that all the roots of* $p(\lambda)$ *are negative or have negative real parts if and only if* $a_1 > 0$*,* $a_2 > 0$*,* $a_3 > 0$*, and* $a_1a_2 > a_3$*.*

Chapter 2

The Mathematical Model and its Derivation

We present a generalized model describing red blood cell dynamics under blood loss.

2.1 Assumptions

- The subject is a healthy adult with sufficient iron levels.
- Only the most essential features of erythropoiesis are considered to reduce model complexity.
- Factors of erythropoiesis vary between individuals and can be accounted for by parameters.
- Cells have a constant differentiation rate concerning EPO.
- Stem cells do not have the ability of self-renewal to maintain cell populations.
- EPO feedback and blood plasma regeneration are instant.
- The immature red blood cell stages can be partitioned into two compartments, EPO-proliferating and non-EPO-proliferating.
- Cell age and sized can be averaged by application of the law of large numbers.

2.2 Derivation

Variables	Description	Units
$R_1(t)$	Stage 1 of precursor cells - proliferating with respect to EPO - at time t	population
$R_2(t)$	Stage 2 of precursor cells - not proliferating with respect to EPO - at time t	population
$R_3(t)$	Mature erythrocytes at time t	population
t	Time in days	time (days)

Table 2.1: Description of variables used in the model.

Functional Forms	Description	Units
$G(R_1)$	Production of precursor erythrocytes	population / time
$F(R_3)$	Feedback regulating erythropoiesis, dependent on blood loss	unitless
$H(R_3)$	Blood loss due to external factors	population / time

Table 2.2: Functional forms used in the model.

Parameters	Description	Units
β	Individual blood regeneration amplifying factor	unitless
k_1, k_2	Transition rates between stages	1/time
μ_1, μ_2, μ_3	Apoptosis rates of stages	1/time
γ	Blood regeneration amplifying factor	1 / time
R_1^0, R_2^0, R_3^0	Population sizes of R_1, R_2, R_3, respectively, at $t = 0$	population

Table 2.3: Parameters used in the model.

The generalized system of ordinary differential equations (2.1) and its initial conditions (2.2) are stated and represented with a schematic in Figure 2.1:

$$\begin{aligned}
\dot{R}_1 &= \beta G(R_1) - \beta k_1 R_1 - \beta \mu_1 R_1 + \gamma F(R_3) R_1 \\
\dot{R}_2 &= \beta k_1 R_1 - \beta \mu_2 R_2 - \beta k_2 R_2 \\
\dot{R}_3 &= \beta k_2 R_2 - \beta \mu_3 R_3 - H(R_3)
\end{aligned} \tag{2.1}$$

$$R_1(0) = R_1^0$$
$$R_2(0) = R_2^0 \tag{2.2}$$
$$R_3(0) = R_3^0$$

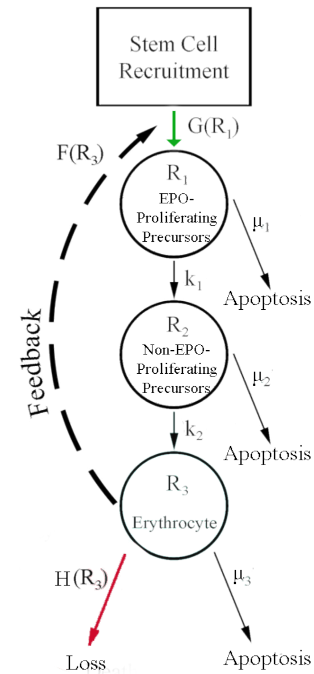

Figure 2.1: Model Schematic

$G(R_1)$ represents the natural growth of the stage one precursors - proliferating with respect to EPO - cells entering the red blood cell line from the bone marrow. k_1R_1 represents the maturation and transition of cells from the EPO-proliferating stage to the non-EPO-proliferating stage. The production of stage one cells is partially dependent on feedback due to EPO, while the later stages are not. μ_1R_1 is the apoptosis rate (natural death rate) of the first stage of precursor cells. $F(R_3)$ is a feedback function which stimulates the production of stage 1 (EPO-proliferating) precursor cells in the bone marrow when the mature erythrocyte population is low due to loss. k_2R_2 represents the maturation of stage two precursors, those not proliferating with respect to EPO, into mature erythrocytes. μ_2R_2 is the apoptosis rate of the second stage of precursors. $H(R_3)$ is a function that models additional blood loss due to external factors such as bloodletting or parasitemia. β and γ vary among individuals, representing differences in erythropoiesis. A low β value corresponds to feedback having a larger influence for a longer amount of time. High values of γ, meanwhile, correspond to faster regeneration of blood loss, but can drive the system into oscillatory dynamics.

2.3 Function Choices

To complete the model (2.1) with initial conditions (2.2) we must define functional choices F, G, and H that will govern the model dynamics of system (2.1) with (2.2).

1) **Recruitment Function** $G(R_1)$:

   $G(R_1)$ models the growth rate of stage 1 precursor cells from the bone marrow. We require that G satisfy certain properties to guarantee a healthy stable population of red blood cells.

   Proposition 1. *For any choice of $G(R_1)$, $G(R_1)$ is a $C^1([0,\infty))$ function such that there exists a $R_1^* > 0$ such that for $R_1 > R_1^*$, $G(R_1)$ is non-increasing and for $R_1 < R_1^*$, $G(R_1)$ is non-decreasing. Additionally,* $\lim_{R_1 \to 0^+} G(R_1) \geq \Gamma \geq \lim_{R_1 \to \infty} G(R_1)$.

   Choices of $G(R_1)$:

   (1) Constant G: $G(R_1) = L$. This choice is utilized by Tetschke et al. [17] as a constant rate of committed stem cells transitioning to R_1.

   (2) Logistic G: $G(R_1) = \alpha R_1(1 - \frac{R_1}{K})$. A logistic model enables growth rates to be more dependent on the size of the existing population of R_1 cells.

   Definition 11. *The* ***logistic model*** *is the differential equation $\frac{dP}{dt} = rP(1 - \frac{P}{K})$, where P is a population, K is the carrying capacity of that population, and r the logistic growth rate of the population. [1]*

2) **Feedback Function** $F(R_3)$:

   For the most part, $F(R_3)$ is a negative feedback function which regulates the production of stage 1 precursor cells (R_1) as a result of changes in the size of the erythrocyte population (R_3) in order to ensure a mammal maintains a healthy stabilized red blood cell count.

   Choices of $F(R_3)$:

   (1) Linear F: $F(R_3) = 1 - \frac{R_3}{s}$. Tetschke et al. [17] defines this monotonically decreasing choice, where s is the mean steady state erythrocyte count. Tetschke et al. [17] models red blood cell regeneration after loss in the context of the myeloproliferative disorder Polycythemia Vera, which causes increased red blood cell production. This choice of F allows for a faster return to the mean steady state erythrocyte count, as F becomes negative for sufficiently large R_3, which enables a faster return to equilibrium when R_3 is over-saturated, which could occur following regeneration.

   (2) Hill-type F: $F(R_3) = \frac{\theta^n}{\theta^n + {R_3}^n}$. Mackey and Glass [10] and Mackey [9] use this hill-type function. This monotonically decreasing function has adjustable slope an inflection point. The authors anticipated use of $n \leq 5$

for this choice. This feedback function allows for much slower return times to equilibrium when compared to the liner F, due to the large tail and asymptotic behavior towards zero of the function as R_3 grows large.

Definition 12. *The **hill equation** has form $f(x) = \frac{x^n}{a+x^n}$, where a and n are parameters.*

Proposition 2. *For any choice of $F(R_3)$, the following properties hold:*

i) $F'(R_3) < 0$ *for all R_3 (F is monotonically decreasing).*

ii) $\lim_{R_3 \to 0} F(R_3) = 1$.

iii) $\lim_{R_3 \to R_3^*} F(R_3) = 0$, *where R_3^* is the steady state value of the R_3 population.*

Remark 1. *In lieu of the fact that $F(R_3$ is a negative feedback function, $\gamma F(R_3)R_1$ must satisfy the following properties:*

i) $\lim_{R_3 \longrightarrow \infty} \gamma F(R_3)R_1 \longrightarrow 0$

ii) As $R_1 \longrightarrow \infty$ and $R_3 \longrightarrow \infty$, $\gamma F(R_3)R_1 \longrightarrow 0$
The growth of R_1 is $O(R_3^{-\eta})$, where $\eta > 1$.

3) **External Loss Function** $H(R_3)$: H is a positive, bounded function which models additional loss due to a given situation.

(1) Constant H: $H(R_3) = A$ can be used in the case of constant, continuous loss. The parameter A has units of population/time.

(2) Indicator H: An indicator function may be used for H in the case of a blood donation or blood letting, where a constant loss occurs over some fixed interval of time.

(3) Piecewise-continuous H: More complicated piecewise functions can be used for H to model blood loss due to the menstrual cycle. An example of such a piecewise-continuous function is given, where the parameter A is the same as above:

$$H(R_3) = \begin{cases} 0 & \text{if } (t \mod 30) < 24 \\ A & \text{else} \end{cases}$$

(4) Sinusoidal H: A sinusoidal H such as $H(R_3) = A|\sin(\pi t/30)|$ could also be used to model blood loss due to the menstrual cycle.

Proposition 3. *We assume that $H(0) = 0$. In the above cases, we have omitted this requirement, as numerical results (in later chapters) with prudent choices of initial conditions and parameters show that $R_3 = 0$ does not occur for the choices of H given above.*

In the presence of malaria parasitemia, H will be a function of R_3 and P, where P is the load of the parasite forms that infect healthy red blood cells. For this case, the size of the system would increase to account for the dynamics of the malaria parasitemia. This will be considered in the future. For the purpose of this thesis, we will consider the cases where $H = 0$ analytically and numerically and consider the scenarios of $H \neq 0$ enumerated above numerically. In Chapters 3 and 4 we will assume $H = 0$ and consider the following four scenarios of F and G:

$$F(R_3) = 1 - \frac{R_3}{s} \qquad G(R_1) = L \tag{2.3}$$

$$F(R_3) = \frac{\theta^n}{\theta^n + {R_3}^n} \qquad G(R_1) = L \tag{2.4}$$

$$F(R_3) = 1 - \frac{R_3}{s} \qquad G(R_1) = \alpha R_1 (1 - \frac{R_1}{K}) \tag{2.5}$$

$$F(R_3) = \frac{\theta^n}{\theta^n + {R_3}^n} \qquad G(R_1) = \alpha R_1 (1 - \frac{R_1}{K}) \tag{2.6}$$

We illustrate the shapes and sensitivity to parameters of these functional forms in Figure 2.2 with parameters listed in Table 2.4.

Parameters	Description	Units
s	Mean steady state erythrocyte count	population
θ	Half-saturation erythrocyte count	population
n	Sensitivity of feedback w.r.t changes in population size	unitless
L	Constant growth rate for R_1	population /time
α	Logistic growth rate	1/time
K	Maximum stimulated size of R_1	population

Table 2.4: Parameters used in the functional forms.

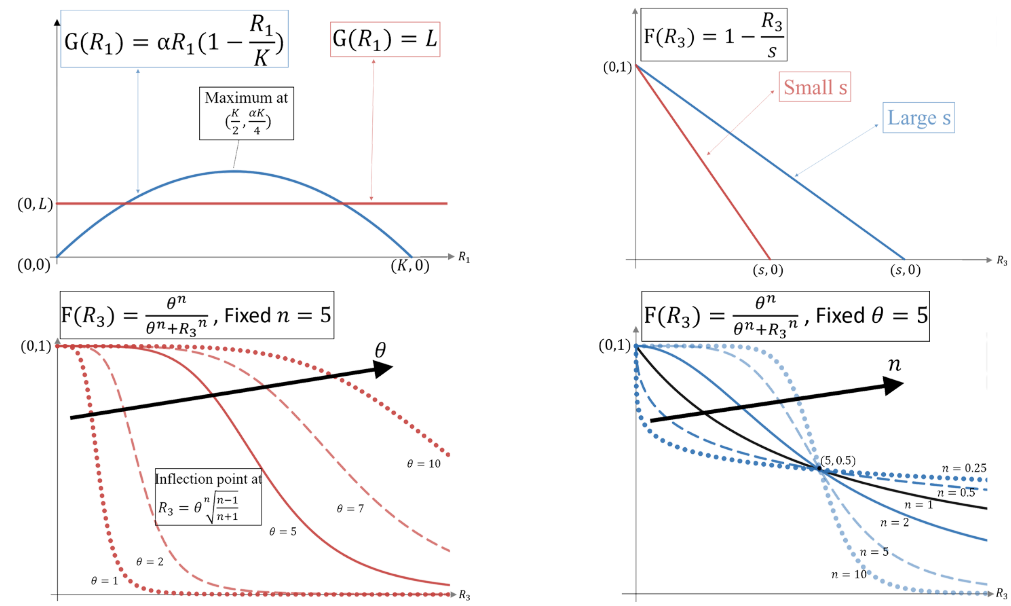

Figure 2.2: Both choices of F and both choices of G given above, illustrating sensitivity to parameters.

2.4 Parameter Estimation

2.4.1 Human Parameters and Maximal Variable Sizes

A healthy 75-kg human adult male is known to have a mean steady state count of $s = 24.98 \times 10^{12}$ circulating erythrocytes and reticulocytes [8] (p. 482), [4], with 3331×10^8 cells per kg of body weight [8]. We establish a range of 18×10^{12} to 31×10^{12} in Table 2.5 to account for fluctuations in individual numbers due to varying weight or sex. β and γ reflect the differences in erythropoiesis among individuals, with β representing the individual blood regeneration amplifying factor independent of fractional blood loss and γ representing the individual blood regeneration amplifying factor dependent on fractional blood loss. In Tetschke et al. [17], a base value of $\beta = 1$ was chosen in the range [0.75,3] and $\gamma = 0.3$ in the range (0,2]. A low β value corresponds to feedback having a larger influence for a longer amount of time. High values of γ, meanwhile, correspond to faster regeneration of blood loss, but can potentially drive the system into oscillatory dynamics.

$\mu_3 = 1/120$ represents the average 120 day lifespan of the mature erythrocyte in humans [8]. $k_1 = 1/8$ and $k_2 = 1/6$ reflect, respectively in humans, the 8 days during which precursor cells are EPO-proliferating (the duration of stage 1 precursors' existence) and the subsequent 6 days during which precursor cells are non-EPO-proliferating (stage 2 precursors) [17] [8]. μ_1 and μ_2 represent the apoptosis rate of the stage 1 and stage 2 precursor cells, respectively, and are assumed to be negligibly 0 in humans by Tetschke et al. [17]. Fuertinger et al. [4], however, suggests that choices of μ_1 as large as 0.35 may be appropriate for CFU-E cells, which we take into account in the corresponding range of [0,0.35] for μ_1. We estimate apoptosis for μ_2 to be similar and give an identical range for this parameter.

L is chosen to provide a constant growth rate of stage 1 precursor cells that will exactly balance the natural death of erythrocytes given by μ_3 when there is no external loss ($H = 0$) and subsequently no feedback ($F = 0$) because the erythrocyte population is at its mean steady state count. This situation corresponds to $\dot{R}_1 = \dot{R}_2 = \dot{R}_3 = 0$ and $R_3 = s$. It implies that $L = \mu_3 s$, assuming $\mu_1 = \mu_2 = 0$. Using the established values and ranges for s and μ_3 given above, we have that $L = 0.21 \times 10^{12}$ on [0.15x10^{12}, 0.26x10^{12}]. K represents the maximal stimulated value of stage 1 precursor cells. We estimate the value of K by first considering the model at a steady state where $H = 0$, $\dot{R}_1 = \dot{R}_2 = \dot{R}_3 = 0$, and $R_3 = s$. In this scenario, assuming $\mu_1 = \mu_2 = 0$, the relationship $R_1 = \frac{\mu_3}{k_1} R_3$ holds, meaning that we can compute the mean steady state value of R_1 in terms of the given parameter value of s. Here, we have a calculated mean steady state count of stage 1 precursor cells in the range of [1.2, 2.07] (x10^{12} cells). To compute an estimate for the maximal stimulated value of stage 1 precursor cells, we multiply this range by 4 to produce a coarse upper bound for use in the logistic function choice of $G(R_1)$. Thus, the estimated value for K is 6.66x10^{12} on [4.8, 8.27] (x10^{12}).

We estimate α, the growth rate of the logistic stage 1 precursor growth function G, from numerical simulation. $\alpha = 0.166$ on the range [0.05, 0.4] produces results in which the steady state erythrocyte count value corresponds to the ranges given above. Finally, n and θ are chosen based on Mackey and Glass [10] and Mackey [9], where θ is the half-saturation value and $n \leq 5$. We choose $n = 5$ with a range of (0, 5], and take $\theta = s/2$, since θ is used in the hill-type function choice of F, which is a function of R_3, a variable which has a corresponding mean steady state count as s. Hence $\theta = 12.5 \times 10^{12}$ on a range of 9×10^{12} to 16×10^{12}.

2.4.2 Mouse Parameters and Maximal Variable Sizes

We next discuss relevant parameters for laboratory mice. A healthy adult laboratory mouse is known to have a mean steady state count of approximately $s = 19 \times 10^9$ circulating erythrocytes and reticulocytes [5], with $7 - 11 \times 10^{12}$ cells per liter of blood [5]. We establish a range of 11×10^9 to 27×10^9 in Table 2.5 to account for fluctuations in individual mouse numbers due to varying weight or age. We assume that β and γ can be kept at the same values as they were for humans, as they represent individual-level amplification factors. $\mu_3 \in [1/52, 1/30]$ represents the 30-52 day lifespan of the mature erythrocyte in mice [5]. For k_1 and k_2 we assume that these transition rates will maintain the same ratio with respect to μ_3 as in humans, thus giving $k_1 \in [15/52, 1/2]$ and $k_2 \in [5/13, 2/3]$ by the values of μ_3 given above. For μ_1 and μ_2 we take a baseline value of 0 but maintain the allowable parameter range to be the same as that of humans, [0, 0.35]. Like in humans, L is chosen from $L = \mu_3 s$, using the ranges for s and μ_3 given above. Therefore, $L = 19/41 \times 10^9$ on [11/52x10^9, 9/10x10^9]. Similarly, K is chosen by $K = 4\frac{\mu_3}{k_1}s$, giving 7.7x10^9 on [2.93, 12.48] (x10^9). We assume α remains the same as in the human model. n and

Human Parameter Ranges				
Parameter	Range of Values	Baseline Value	Dimension	Reference
μ_1	[0,0.35]	0	1/day	Fuertinger et al. [4]
μ_2	[0,0.35]	0	1/day	Estimated
μ_3	1/120	1/120	1/day	Tetschke et al. [17]
k_1	1/8	1/8	1/day	Tetschke et al. [17]
k_2	1/6	1/6	1/day	Tetschke et al. [17]
γ	(0,2]	0.3	1/day	Tetschke et al. [17]
s	[18,31]	24.98	population (x10^{12} cells)	Tetschke et al. [17], Fuertinger et al. [4]
β	[0.75,3]	1	unitless	Tetschke et al. [17]
L	[0.15, 0.26]	0.21	population (x10^{12} cells)	Tetschke et al. [17]
θ	[9,16]	12.5	population (x10^{12} cells)	Mackey [9]
n	(0,5]	5	unitless	Mackey [9]
α	[0.05,0.4]	0.166	1/day	Estimated
K	[4.8,8.27]	6.66	population (x10^{12} cells)	Estimated

Table 2.5: Range and baseline values for parameters and their dimensional units within a healthy adult human.

Mouse Parameter Ranges

Parameter	Range of Values	Baseline Value	Dimension	Reference
μ_1	[0,0.35]	0	1/day	Fuertinger et al. [4], estimated
μ_2	[0,0.35]	0	1/day	Estimated
μ_3	[1/52, 1/30]	1/41	1/day	Hedrich [5]
k_1	[15/52, 1/2]	15/41	1/day	Estimated
k_2	[5/13, 2/3]	20/41	1/day	Estimated
γ	(0,2]	0.3	1/day	Tetschke et al. [17]
s	[11,27]	19	population (x10^9 cells)	Hedrich [5]
β	[0.75,3]	1	unitless	Tetschke et al. [17]
L	[11/52, 9/10]	19/41	population (x10^9 cells)	Tetschke et al. [17]
θ	[5.5,13.5]	9.5	population (x10^9 cells)	Mackey [9]
n	(0,5]	5	unitless	Mackey [9]
α	[0.05,0.4]	0.166	1/day	Estimated
K	[2.93, 12.48]	7.7	population (x10^9 cells)	Estimated

Table 2.6: Range and baseline values for parameters and their dimensional units within a healthy mouse.

θ are chosen analogously to the human parameters based on Mackey and Glass [10] and Mackey [9]. We choose $n = 5$ with a range of $(0, 5]$, and take $\theta = s/2$, hence $\theta = 9.5 \times 10^9$ on a range of 5.5×10^9 to 13.5×10^9.

Chapter 3

Mathematical Analyses

3.1 Basic Model Properties

3.1.1 Positive Invariance

Theorem 1. *The system (2.1) is positively invariant, that is, for all solutions $\vec{R}(t)$ of (2.1), if $\vec{R}(0) \in \mathbb{R}^3_+$, then $\vec{R}(t) \in \mathbb{R}^3_+ \ \forall\ t > 0$.*

Proof. We use the proof technique of Woldegerima et al. [19] and will show that $\dot{R}_1$, $\dot{R}_2$, and $\dot{R}_3$ are nonnegative at $\vec{R} = \mathbf{0}$ and on the $R_1 = 0$, $R_2 = 0$, and $R_3 = 0$ planes, in order to demonstrate that the vector field points inward, so no solution beginning in $\mathbb{R}^3_+$ becomes negative.

When $\vec{R} = \mathbf{0}$, $\dot{R}_2 = (0)\beta k_1 - (0)\beta\mu_2 - \beta k_2(0) = 0$ and $\dot{R}_3 = (0)\beta k_2 - (0)\beta\mu_3 - H(0) = 0$ (Proposition 3), while $\dot{R}_1 = \beta G(0) - (0)\beta k_1 - (0)\beta\mu_1 + (0)\gamma F(0) = \beta G(0) \geq 0$ (Proposition 1). Thus when $\vec{R} = \mathbf{0}$, R_1, R_2, and R_3 are nondecreasing.

On the $R_1 = 0$ plane, for nonnegative values of R_2 and R_3, $\dot{R}_1 = \beta G(0) - (0)\beta k_1 - (0)\beta\mu_1 + (0)\gamma F(R_3) = \beta G(0) \geq 0$ (Proposition 1). On the $R_2 = 0$ plane, for nonnegative values of R_1 and R_3, $\dot{R}_2 = \beta k_1 R_1 - (0)\beta\mu_2 - (0)\beta k_2 = \beta k_1 R_1 \geq 0$. On the $R_3 = 0$ plane, for nonnegative values of R_1 and R_2, $\dot{R}_3 = \beta k_2 R_2 - (0)\beta\mu_3 - H(0) = \beta k_2 R_2 \geq 0$ (Proposition 3). Thus the region $\mathbb{R}^3_+$ is positively invariant and attracting for the system (2.1), as we have shown that no solution to (2.1) which starts in $\mathbb{R}^3_+$ passes out of $\mathbb{R}^3_+$. $\square$

3.1.2 Positivity of Solutions

Theorem 2. *All solutions to (2.1) with initial conditions in $\mathbb{R}^3_+$ are positive.*

Proof. Let $\vec{R(t)} = (R_1(t), R_2(t), R_3(t))$ be an arbitrary solution of (2.1) with initial conditions in $\mathbb{R}^3_+$. We proceed by contradiction for each R_i, again using a proof technique from Woldegerima et al. [19]. For R_1, assume for some $t_1 > 0$, $R_1(t_1) = 0$, $\dot{R}_1(t_1) < 0$, and $R_2(t)$ and $R_3(t)$ are strictly positive for all $t \in (0, t_1)$. But $\dot{R}_1(t_1) = \beta G(0) - (0)\beta k_1 - (0)\beta\mu_1 R_1 + (0)\gamma F(R_3) = \beta G(0) \geq 0$, a contradiction (Proposition 1). Thus $R_1(t) > 0 \ \forall\ t \geq 0$. For R_2, assume for some $t_2 > 0$,

$R_2(t_2) = 0$, $\dot{R}_2(t_2) < 0$, and $R_1(t)$ and $R_3(t)$ are strictly positive for all $t \in (0, t_2)$. But from the second equation of (2.1), $\dot{R}_2(t_2) = \beta k_1 R_1 - (0)\beta\mu_2 - (0)\beta k_2 > 0$, as $R_1(t) > 0$, a contradiction. Thus $R_2(t) > 0 \; \forall \; t \geq 0$. For R_3, assume for some $t_3 > 0$, $R_3(t_3) = 0$, $\dot{R}_3(t_3) < 0$, and $R_1(t)$ and $R_2(t)$ are strictly positive for all $t \in (0, t_3)$. But $\dot{R}_3(t_3) = \beta k_2 R_2 - (0)\beta\mu_3 - H(0) = \beta k_2 R_2 > 0$, a contradiction (Proposition 3). Thus $R_3(t) > 0 \; \forall \; t \geq 0$. Thus all solutions to (2.1) with initial conditions in $\mathbb{R}^3_+$ are positive. □

3.1.3 Boundedness of Solutions

Theorem 3. *All solutions to (2.1) with initial conditions in $\mathbb{R}^3_+$ are bounded.*

Proof. Let $\vec{R(t)} = (R_1(t), R_2(t), R_3(t))$ be an arbitrary solution of (2.1) with initial conditions in $\mathbb{R}^3_+$. We proceed by contradiction for R_1 and directly compute the bound for R_2 and R_3, again using a proof technique from Woldegerima et al [19]. For R_1, assume that $R_1(t)$ is unbounded. Then for any choice of $M \in \mathbb{R}$, there exists some $t_4 > 0$ such that $R_1(t_4) > M$ and $\dot{R}_1 > 0$ in some neighborhood J near t_4 by continuity of the solution. On J, the following inequality holds:

$$0 < \dot{R}_1 = \beta G(R_1) - \beta(k_1 + \mu_1)R_1 + \gamma F(R_3)R_1 \leq \beta G_M - \beta(k_1 + \mu_1)R_1 + \gamma F(R_3)R_1 \tag{3.1}$$

Where $G_M = \max\limits_{R_1 \in \mathbb{R}_+} G(R_1)$, as $G(R_1)$ is positive and bounded by Proposition 1. In fact, for the two functional choices for G given in Chapter 2.3, we have:

$$G_M = \begin{cases} L & \text{if } G(R_1) = L \\ \frac{\alpha K}{4} & \text{if } G(R_1) = \alpha R_1(1 - \frac{R_1}{K}) \end{cases}$$

For choice of M sufficiently large, $\beta G_M < \beta k_1 R_1$ in J, implying that the $\gamma F(R_3)R_1$ term must be large to achieve the positivity of the expression. However, by Remark 1, $\gamma F(R_3)R_1$ will be driven to zero as $R_1 \longrightarrow \infty$, hence (3.1) cannot be positive, a contradiction. Thus R_1 is bounded.

For R_2, we refer to the second equation of (2.1), and denote the upper bound of $R_1(t)$ as A_1. The following inequality arises:

$$\dot{R}_2 = \beta k_1 R_1 - \beta(k_2 + \mu_2)R_2 \leq \beta k_1 A_1 - \beta(k_2 + \mu_2)R_2 \tag{3.2}$$

Using a proof technique of Woldegerima et al [19], we solve the differential equation presented in (3.2) to obtain the following inequality:

$$R_2(t) \leq \frac{k_1 A_1}{(k_2 + \mu_2)} + C_1 e^{-\beta(k_2+\mu_2)t} \tag{3.3}$$

C_1 is a positive constant determined by the chosen initial conditions on (2.1). Regardless of the value of C_1, as t goes to infinity, the limit supremum of $R_2(t)$ is bounded above by $\frac{k_1 A_1}{(k_2+\mu_2)}$. Thus R_2 is bounded; we denote its upper bound as A_2.

For R_3, the third equation of (2.1) and the positivity and boundedness of H give rise to the following inequality:

$$\dot{R}_3 = \beta k_2 R_2 - \beta\mu_3 R_3 - H(R_3) \leq \beta k_2 A_2 - \beta\mu_3 R_3 \tag{3.4}$$

Solving the differential equation in (3.4) gives the inequality:

$$R_3(t) \leq \frac{k_2 A_2}{\mu_3} + C_2 e^{-\beta\mu_3 t} \tag{3.5}$$

C_2 is a positive constant determined by the chosen initial conditions on (2.1). Regardless of the value of C_2, as t goes to infinity, the limit supremum of $R_3(t)$ is bounded above by $\frac{k_2 A_2}{\mu_3}$. Thus R_3 is bounded and all solutions $\vec{R(t)}$ of (2.1) with initial conditions in $\mathbb{R}^3_+$ are bounded. □

3.1.4 Uniqueness of Solutions

Theorem 4. *All solutions to (2.1) with initial conditions in $\mathbb{R}^3_+$ are unique.*

Proof. Denote $\vec{\Phi}(R_1, R_2, R_3) = \dot{R}$ from (2.1). Every function with bounded first partial derivatives is Lipschtiz. The partial derivatives of $\vec{\Phi}$ are as follows:

$$\begin{aligned}
\frac{\partial\vec{\Phi}}{\partial R_1} &= (\beta G'(R_1) - \beta k_1 - \beta\mu_1 + \gamma F(R_3),\ \beta k_1,\ 0)^T \\
\frac{\partial\vec{\Phi}}{\partial R_2} &= (0,\ -\beta k_2 - \beta\mu_2,\ \beta k_2)^T \\
\frac{\partial\vec{\Phi}}{\partial R_3} &= (\gamma R_1 F'(R_3),\ 0,\ -\beta\mu_3 - H'(R_3))^T
\end{aligned} \tag{3.6}$$

Using the infinity norm, we have:

$$||\frac{\partial\vec{\Phi}}{\partial R_1}||_\infty = \max_{\vec{R}} |\beta G'(R_1) - \beta k_1 - \beta\mu_1 + \gamma F(R_3), \beta k_1|$$

But as $F(R_3) \leq 1$ and, for the two functional choices for G given in Chapter 2.3 we have:

$$G'(R_1) = \begin{cases} 0 & \text{if } G(R_1) = L \\ \alpha - \frac{2\alpha R_1}{K} & \text{if } G(R_1) = \alpha R_1(1 - \frac{R_1}{K}) \end{cases}$$

We see that $G'(R_1)$ is bounded since we have shown that $R_1(t)$, $R_2(t)$, and $R_3(t)$ are positive and bounded, therefore $||\frac{\partial\vec{\Phi}}{\partial R_1}||_\infty$ is finite. Clearly $\frac{\partial\vec{\Phi}}{\partial R_2}$ is bounded as it is a constant vector. Finally, we have:

$$||\frac{\partial\vec{\Phi}}{\partial R_3}||_\infty = \max_{\vec{R}} |\gamma R_1 F'(R_3), -\beta\mu_3 - H'(R_3)|$$

For the choices of H given in Chapter 2.3, H' is certainly bounded, as constant functions and the sine function have bounded derivatives. The derivatives of the choices of F given in Chapter 2.3 are:

$$F'(R_3) = \begin{cases} -\frac{1}{s} & \text{if } F(R_3) = 1 - \frac{R_3}{s} \\ -\frac{\theta^n n {R_3}^{n-1}}{(\theta^n + {R_3}^n)^2} & \text{if } F(R_3) = \frac{\theta^n}{\theta^n + {R_3}^n} \end{cases}$$

As R_3 is positive and bounded, $F'(R_3)$ is also bounded, hence $||\frac{\partial \vec{\Phi}}{\partial R_3}||_\infty$ is finite. Therefore the partial derivatives of $\vec{\Phi}$ are bounded. Thus (2.1) is Lipschitz continuous, and therefore by the existence and uniqueness theorem has a unique solution. □

3.1.5 Monotonicity

Theorem 5. *The system (2.1) is not a monotone system.*

Proof. If the Jacobian matrix of a system is a Metzler matrix, then that system is monotone [16]. A Metzler matrix is a matrix with all non-diagonal terms nonnegative. The Jacobian matrix of (2.1) is given in (3.7):

$$J(R_1, R_2, R_3) = \begin{bmatrix} \beta G'(R_1) - \beta k_1 - \beta\mu_1 + \gamma F(R_3) & 0 & \gamma F'(R_3) R_1 \\ \beta k_1 & -\beta k_2 - \beta\mu_2 & 0 \\ 0 & \beta k_2 & -\beta\mu_3 - H'(R_3) \end{bmatrix} \tag{3.7}$$

Since $F(R_3)$ is monotonically decreasing (Proposition 2), we know $F'(R_3) < 0$, hence the top right entry in the Jacobian matrix is negative. Therfore the Jacobian is not a Metzler matrix, so (2.1) is not a monotone system.

□

3.2 Nondimensionalization

We nondimensionalize the system (2.1) to give a more complete understanding of the system by reducing the number of parameters. For each of the four scenarios for F and G presented in Section 2.3, we seek to find appropriate values of T_0, A, B, and C such that the variables τ, r_1, r_2, and r_3 given in (3.8) are unitless and reduce the number of parameters in the system (2.1).

$$\tau = \frac{t}{T_0}, \quad r_1 = \frac{R_1}{A}, \quad r_2 = \frac{R_2}{B}, \quad r_3 = \frac{R_3}{C} \tag{3.8}$$

Substituting from the expressions in (3.8), the system (2.1) is transformed into

(3.9).

$$
\begin{aligned}
\frac{A}{T_0}\frac{dr_1}{d\tau} &= \beta G(Ar_1) - \beta k_1 Ar_1 - \beta\mu_1 Ar_1 + \gamma F(Cr_3)Ar_1 \\
\frac{B}{T_0}\frac{dr_2}{d\tau} &= \beta k_1 Ar_1 - \beta\mu_2 Br_2 - \beta k_2 Br_2 \\
\frac{C}{T_0}\frac{dr_3}{d\tau} &= \beta k_2 Br_2 - \beta\mu_3 Cr_3 - H(Cr_3)
\end{aligned}
\tag{3.9}
$$

Further algebraic manipulation of the system in (3.9) yields (3.10).

$$
\begin{aligned}
\frac{dr_1}{d\tau} &= \beta\frac{T_0}{A}G(Ar_1) - \beta k_1 T_0 r_1 - \beta\mu_1 T_0 r_1 + \gamma F(Cr_3)T_0 r_1 \\
\frac{dr_2}{d\tau} &= \frac{\beta k_1 A T_0}{B} r_1 - \beta\mu_2 T_0 r_2 - \beta k_2 T_0 r_2 \\
\frac{dr_3}{d\tau} &= \frac{\beta k_2 B T_0}{C} r_2 - \beta\mu_3 T_0 r_3 - \frac{T_0}{C}H(Cr_3)
\end{aligned}
\tag{3.10}
$$

We nondimensionalize time by scaling by the lifespan of the mature red blood cell, that is, by taking $T_0 = \frac{1}{\beta\mu_3}$. Plugging this value of T_0 into the system (3.10) yields (3.11).

$$
\begin{aligned}
\frac{dr_1}{d\tau} &= \frac{1}{A\mu_3}G(Ar_1) - \frac{k_1}{\mu_3}r_1 - \frac{\mu_1}{\mu_3}r_1 + \frac{\gamma}{\beta\mu_3}F(Cr_3)r_1 \\
\frac{dr_2}{d\tau} &= \frac{k_1 A}{\mu_3 B}r_1 - \frac{\mu_2}{\mu_3}r_2 - \frac{k_2}{\mu_3}r_2 \\
\frac{dr_3}{d\tau} &= \frac{k_2 B}{\mu_3 C}r_2 - r_3 - \frac{1}{\beta\mu_3 C}H(Cr_3)
\end{aligned}
\tag{3.11}
$$

Letting $B = \frac{k_1 A}{\mu_3}$ and defining the nondimensional parameters δ_1, δ_2, ρ, and a as in (3.14), the system (3.11) can be further simplified to (3.12).

$$
\begin{aligned}
\dot{r}_1 &= \frac{1}{A\mu_3}G(Ar_1) - \delta_1 r_1 + \rho F(Cr_3)r_1 \\
\dot{r}_2 &= r_1 - \delta_2 r_2 \\
\dot{r}_3 &= ar_2 - r_3 - \frac{1}{\beta\mu_3 C}H(Cr_3)
\end{aligned}
\tag{3.12}
$$

Referencing each of the cases given in Section 2.3, we determine values for A and C that further reduce the number of parameters in use. These values result in unitless functions f, g, and h, which are rescalings of F, G, and H. These choices are summarized in (3.13), where ω is given in (3.14).

$$f(r_3) = \begin{cases} 1 - r_3 & C = s \\ \frac{1}{1+r_3^n} & C = \theta \end{cases} \quad g(r_1) = \begin{cases} 1 & A = \frac{L}{\mu_3} \\ \omega r_1(1-r_1) & A = K \end{cases} \quad h(r_3) = \frac{1}{C\beta\mu_3} H(Cr_3) \tag{3.13}$$

$$\delta_1 = \frac{k_1 + \mu_1}{\mu_3} \qquad \delta_2 = \frac{k_2 + \mu_2}{\mu_3} \qquad \rho = \frac{\gamma}{\beta\mu_3} \qquad \omega = \frac{\alpha}{\mu_3} \tag{3.14}$$

$$a = \begin{cases} \frac{k_1 k_2 L}{\mu_3^3 s} & \text{if } f(r_3) = 1 - r_3 \text{ and } g(r_1) = 1 \\ \frac{k_1 k_2 L}{\mu_3^3 \theta} & \text{if } f(r_3) = \frac{1}{1+r_3^n} \text{ and } g(r_1) = 1 \\ \frac{k_1 k_2 K}{\mu_3^2 s} & \text{if } f(r_3) = 1 - r_3 \text{ and } g(r_1) = \omega r_1(1-r_1) \\ \frac{k_1 k_2 K}{\mu_3^2 \theta} & \text{if } f(r_3) = \frac{1}{1+r_3^n} \text{ and } g(r_1) = \omega r_1(1-r_1) \end{cases}$$

Then, finally, the original system (2.1) is transformed to the unitless system in (3.15) through nondimensionalization:

$$\begin{aligned} \dot{r}_1 &= g(r_1) - \delta_1 r_1 + \rho f(r_3) r_1 \\ \dot{r}_2 &= r_1 - \delta_2 r_2 \\ \dot{r}_3 &= a r_2 - r_3 - h(r_3) \end{aligned} \tag{3.15}$$

With initial conditions given by (3.16):

$$\begin{aligned} r_1(0) &= \frac{R_1^0}{A} = r_1^0 \\ r_2(0) &= \frac{R_2^0 \mu_3}{k_1 A} = r_2^0 \\ r_3(0) &= \frac{R_3^0}{C} = r_3^0 \end{aligned} \tag{3.16}$$

By (3.13), the nondimensionalized forms of (2.3), (2.4), (2.5), and (2.6), respectively, are restated as follows:

$$f(r_3) = 1 - r_3 \qquad g(r_1) = 1 \qquad h(r_3) = 0 \tag{3.17}$$

$$f(r_3) = \frac{1}{1+r_3^n} \qquad g(r_1) = 1 \qquad h(r_3) = 0 \tag{3.18}$$

$$f(r_3) = 1 - r_3 \qquad g(r_1) = \omega r_1(1-r_1) \qquad h(r_3) = 0 \tag{3.19}$$

$$f(r_3) = \frac{1}{1 + r_3^n} \qquad\qquad g(r_1) = \omega r_1(1 - r_1) \qquad\qquad h(r_3) = 0 \tag{3.20}$$

In Table 3.1 we state the new, nondimensionalized parameters for the parameters given in Table 2.5.

Nondimensionalized Human Parameter Ranges		
Parameters	Range of Values	Baseline Value
δ_1	[15, 57]	15
δ_2	[20, 62]	20
ρ	[0, 240]	36
ω	[6, 48]	19.92
n	(0, 5]	5
a (in the case of (3.17))	[174.19, 520]	302.64
a (in the case of (3.18))	[337.5, 1040]	604.8
a (in the case of (3.19))	[46.45, 137.83]	79.98
a (in the case of (3.20))	[90, 275.67]	159.84

Table 3.1: Ranges and baseline values for the nondimensional parameters for a healthy adult human, using Table 2.5 and Chapter 3.2.

3.3 Existence of Steady States when $H = 0$

For each of the below cases, we seek to find the steady state values $\vec{r}^* = (r_1^*, r_2^*, r_3^*)$ of the nondimensionalized system (3.15) for specific choices of f and g with $h = 0$. Ultimately, this results in solving the system of equations:

$$\begin{aligned} 0 &= g(r_1^*) - \delta_1 r_1^* + \rho f(r_3^*) r_1^* \\ 0 &= r_1^* - \delta_2 r_2^* \\ 0 &= a r_2^* - r_3^* \end{aligned} \tag{3.21}$$

The last two equations in (3.21) yield the equality (3.22) regardless of choice of f and g.

$$r_3^* = a r_2^* = \frac{a}{\delta_2} r_1^* \qquad\qquad r_2^* = \frac{1}{\delta_2} r_1^* \tag{3.22}$$

Substitution of the relationship (3.22) into the system at equilibrium (3.21) reduces the problem of finding a steady state $\vec{r}^*$ for the system (3.15) to the solution of the single variable problem given in (3.23).

$$0 = g(r_1^*) - \delta_1 r_1^* + \rho f(\frac{a}{\delta_2} r_1^*) r_1^* \tag{3.23}$$

3.3.1 Existence of Case 1: Linear F, Constant G

In this case we have $f(r_3) = 1 - r_3$ and $g(r_1) = 1$. Substitution into (3.23) yields:

$$1 - \delta_1 r_1^* + \rho(1 - \frac{a}{\delta_2} r_1^*) r_1^* = 1 + (\rho - \delta_1) r_1^* - \frac{\rho a}{\delta_2}(r_1^*)^2 = 0 \tag{3.24}$$

In all scenarios, there is only one positive steady state, where r_1^* given by (3.25) and $\vec{r}^*$ is given in (3.26) by use of (3.22).

$$r_1{}^* = \frac{\rho - \delta_1 + \sqrt{(\rho - \delta_1)^2 + 4\rho \frac{a}{\delta_2}}}{2\rho \frac{a}{\delta_2}} \tag{3.25}$$

$$\vec{r}^* = (r_1^*, r_2^*, r_3^*) = (\rho - \delta_1 + \sqrt{(\rho - \delta_1)^2 + 4\rho \frac{a}{\delta_2}})(\frac{1}{2\rho \frac{a}{\delta_2}}, \frac{1}{2\rho a}, \frac{1}{2\rho}) \tag{3.26}$$

We summarize the existence result for this case in Theorem 6 below.

Theorem 6. ***Existence of Steady State for Case 1:***
The system (3.15) together with initial conditions (3.16) and functional choices (3.17) has a unique, positive steady state for all positive parameter values, defined by (3.26) as:

$$\vec{r}^* = (r_1^*, r_2^*, r_3^*) = (\rho - \delta_1 + \sqrt{(\rho - \delta_1)^2 + 4\rho \frac{a}{\delta_2}})(\frac{1}{2\rho \frac{a}{\delta_2}}, \frac{1}{2\rho a}, \frac{1}{2\rho})$$

3.3.2 Existence of Case 2: Hill-type F, Constant G

In this case we have $f(r_3) = \frac{1}{1+r_3^n}$ and $g(r_1) = 1$. Substitution into (3.23) yields:

$$1 - \delta_1 r_1^* + \rho \frac{1}{1 + (\frac{a}{\delta_2} r_1^*)^n} r_1^* = 0 \tag{3.27}$$

Rearrangement of terms transforms (3.27) to (3.28).

$$-\delta_1 \left(\frac{a}{\delta_2}\right)^n r_1{}^{n+1} + \left(\frac{a}{\delta_2}\right)^n r_1{}^n + (\rho - \delta_1) r_1 + 1 = 0 \tag{3.28}$$

For positive-integer-valued n, Descartes' rule of signs implies that (3.28) will have exactly 1 positive real root if $(\rho - \delta_1) > 0$. Otherwise, (3.28) could have 1 or 3 positive real roots. We summarize this result for this case in Theorem 7 below.

Theorem 7. ***Existence of Steady State for Case 2:***
A necessary condition for the system (3.15) together with initial conditions (3.16) and functional choices (3.18) to have exactly one positive steady state is $(\rho - \delta_1) > 0$. If $(\rho - \delta_1) \leq 0$, there are either one or three positive steady states.

To understand which parameter values cause r_1^* to fall within the ranges given by our nondimensionalized human parameter choices from Table 3.1 and to determine behavior when $(\rho - \delta_1) \leq 0$, we generate several plots in MATLAB for varying choices of the human parameters n, a, and ρ. Results for mice follow analogously. Finding r_1^* by finding the roots of the polynomial given in (3.28) is equivalent to finding the intersection point or points of the graphs of $U(r_1) = \delta_1 \left(\frac{a}{\delta_2}\right)^n {r_1}^{n+1} - \left(\frac{a}{\delta_2}\right)^n {r_1}^n$ and $V(r_1) = (\rho - \delta_1)r_1 + 1$. Graphically we can see the existence of r_1^* within the determined ranges in Figure 3.1.

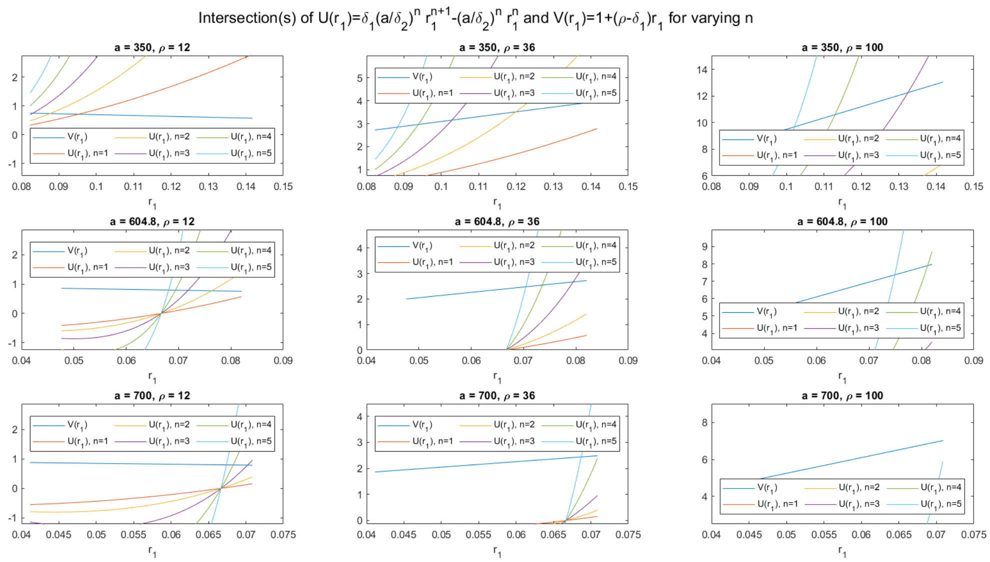

Figure 3.1: Graphs showing the intersection points of U and V for varying human parameter values of n, a, and ρ to demonstrate the existence of r_1^* for case 2: hill-type f, constant g.

Further numerical analysis indicates that at most 1 root will exist for $(\rho - \delta_1) \leq 0$ within the biologically feasible ranges for r_1 given by the parameter choices. As can be seen in the bottom right of Figure 3.1, for certain parameter values - in this case $a = 700$, $\rho = 100$, $n = 5$, r_1^* is not in the desired range - U and V do not intersect within the desired domain of r_1.

Remark 2. *For the parameters given in Tables 2.5 and 2.6, the system (3.15) together with initial conditions (3.16) and functional choices (3.18) has exactly one positive steady state.*

3.3.3 Existence of Case 3: Linear F, Logistic G

In this case we have $f(r_3) = 1 - r_3$ and $g(r_1) = \omega r_1(1 - r_1)$. Substitution into (3.23) yields:

$$\omega r_1^*(1 - r_1^*) - \delta_1 r_1^* + \rho(1 - \frac{a}{\delta_2} r_1^*) r_1^* = 0 \tag{3.29}$$

$$\implies r_1^* = 0 \text{ or } {r_1}^* = \frac{\rho - \delta_1 + \omega}{\omega + \rho\frac{a}{\delta_2}} \text{ if } (\rho - \delta_1 + \omega) > 0$$

There is always a trivial steady state $\vec{r^*} = (0,0,0)$, corresponding to $r_1^* = 0$. If $(\rho - \delta_1 + \omega) > 0$, there is also a positive steady state given by (3.30), using (3.22).

$$\vec{r^*} = (r_1^*, r_2^*, r_3^*) = (\frac{\rho - \delta_1 + \omega}{\omega + \rho\frac{a}{\delta_2}})(1, \frac{1}{\delta_2}, \frac{a}{\delta_2}) \tag{3.30}$$

We summarize the existence result for this case in Theorem 8 below.

Theorem 8. ***Existence of Steady State for Case 3:***

The system (3.15) together with initial conditions (3.16) and functional choices (3.19) has a trivial steady state for all positive parameter values and a unique, positive steady state given by (3.30) and restated below exactly when $(\rho - \delta_1 + \omega) > 0$.

$$\vec{r^*} = (r_1^*, r_2^*, r_3^*) = (\frac{\rho - \delta_1 + \omega}{\omega + \rho\frac{a}{\delta_2}})(1, \frac{1}{\delta_2}, \frac{a}{\delta_2})$$

Remark 3. *The trivial steady state given in Theorem 8 corresponds to death in the mammal and biologically is a steady state that is undesirable for the system to be at.*

3.3.4 Existence of Case 4: Hill-type F, Logistic G

In this case we have $f(r_3) = \frac{1}{1+r_3^n}$ and $g(r_1) = \omega r_1(1 - r_1)$. Substitution into (3.23) yields:

$$\omega r_1^*(1 - r_1^*) - \delta_1 r_1^* + \rho\frac{1}{1 + (\frac{a}{\delta_2}r_1^*)^n}r_1^* = 0 \tag{3.31}$$

Rearrangement of terms transforms (3.31) to (3.32).

$$-\omega\left(\frac{a}{\delta_2}\right)^n {r_1}^{n+2} + (\omega - \delta_1)\left(\frac{a}{\delta_2}\right)^n {r_1}^{n+1} - \omega {r_1}^2 + (\rho + \omega - \delta_1)r_1 = 0 \tag{3.32}$$

For positive-integer-valued n, Descartes' rule of signs implies that (3.32) will have 1 or 3 positive real roots if $(\omega - \delta_1) > 0$. In the case of $\delta_1 > \omega$ and $(\rho+\omega) > \delta_1$, (3.32) will have 1 positive real root. In the case of $\delta_1 \geq (\rho + \omega)$, (3.32) will have no positive real roots. We summarize this result for this case in Theorem 9 below.

Theorem 9. ***Existence of Steady State for Case 4:***

The system (3.15) together with initial conditions (3.16) and functional choices (3.20) has a trivial steady state for all positive parameter values.

A necessary condition for the system (3.15) together with initial conditions (3.16) and functional choices (3.20) to have at least one positive steady state is $\delta_1 < (\rho+\omega)$. If, in addition to $\delta_1 < (\rho + \omega)$, both $\delta_1 > \omega$ and $(\rho + \omega) > \delta_1$ are satisfied, then there will be exactly one positive steady state. On the other hand, if $(\omega - \delta_1) > 0$ in addition to $\delta_1 < (\rho + \omega)$, then there are either one or three positive steady states. If $\delta_1 \geq (\rho + \omega)$, there are no positive steady states.

Factoring out r_1^* from (3.32), we see that further roots correspond to the intersection points of the graphs of $U(r_1) = \omega\left(\frac{a}{\delta_2}\right)^n {r_1}^{n+1} - (\omega - \delta_1)\left(\frac{a}{\delta_2}\right)^n {r_1}^n$ and $V(r_1) = -\omega r_1 + (\rho + \omega - \delta_1)$. We generate several plots in MATLAB in figures 3.2, 3.3, and 3.4 to explore the existence of the intersection points of the graphs of U and V for varying choices of n, ω, ρ, and a given by Table 3.1. In certain cases, U and V do not intersect within the desired domain of r_1. However, we see that in figures 3.2, 3.3, and 3.4, for the ideal human parameter values, given in the center panel of each figure, intersection points exist in the desired domain. Further numerical analysis indicates that, given the established parameter ranges, at most one root will exist with the biologically feasible ranges for r_1 given by the parameter values for all other parameter choices given within their respective ranges. Therefore, a situation with 3 positive real roots will never arise in practice.

Remark 4. *For the parameters given in Tables 2.5 and 2.6, the system (3.15) together with initial conditions (3.16) and functional choices (3.20) has either one or zero positive steady states.*

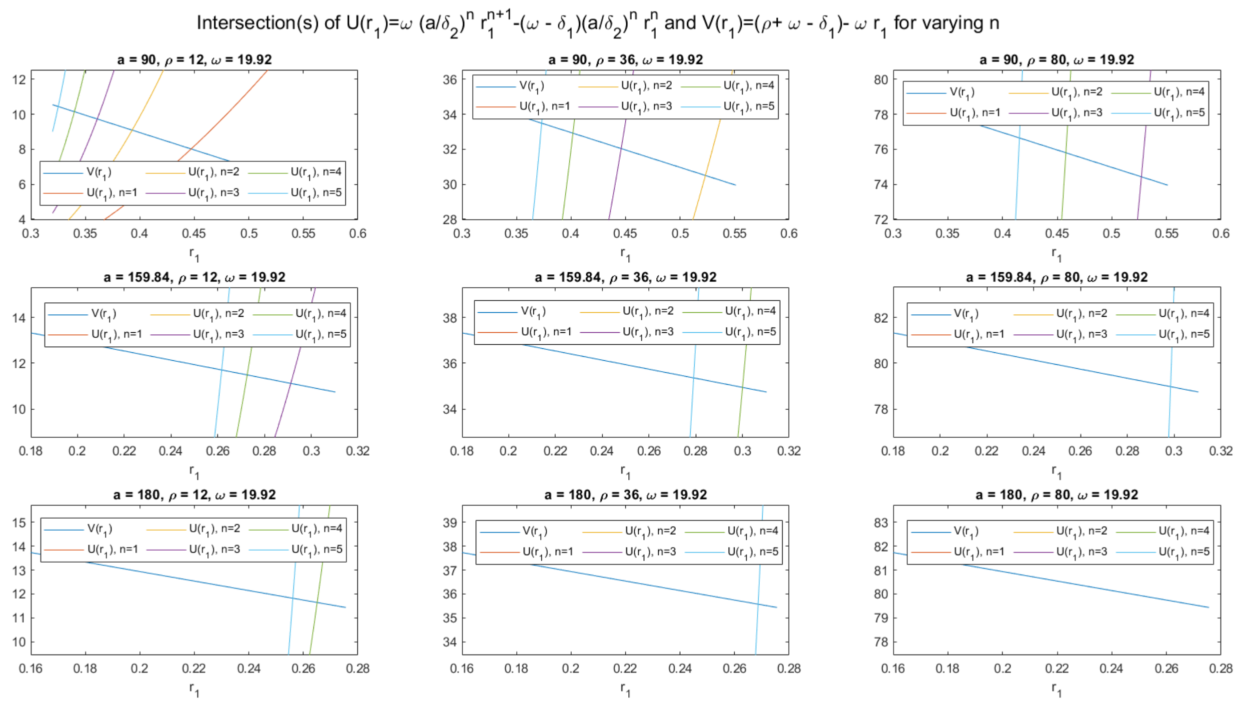

Figure 3.2: Graphs showing the intersection points of U and V for varying human parameter values of n, a, and ρ with ω constant to demonstrate the existence of r_1^* for case 4: hill-type f, logistic g.

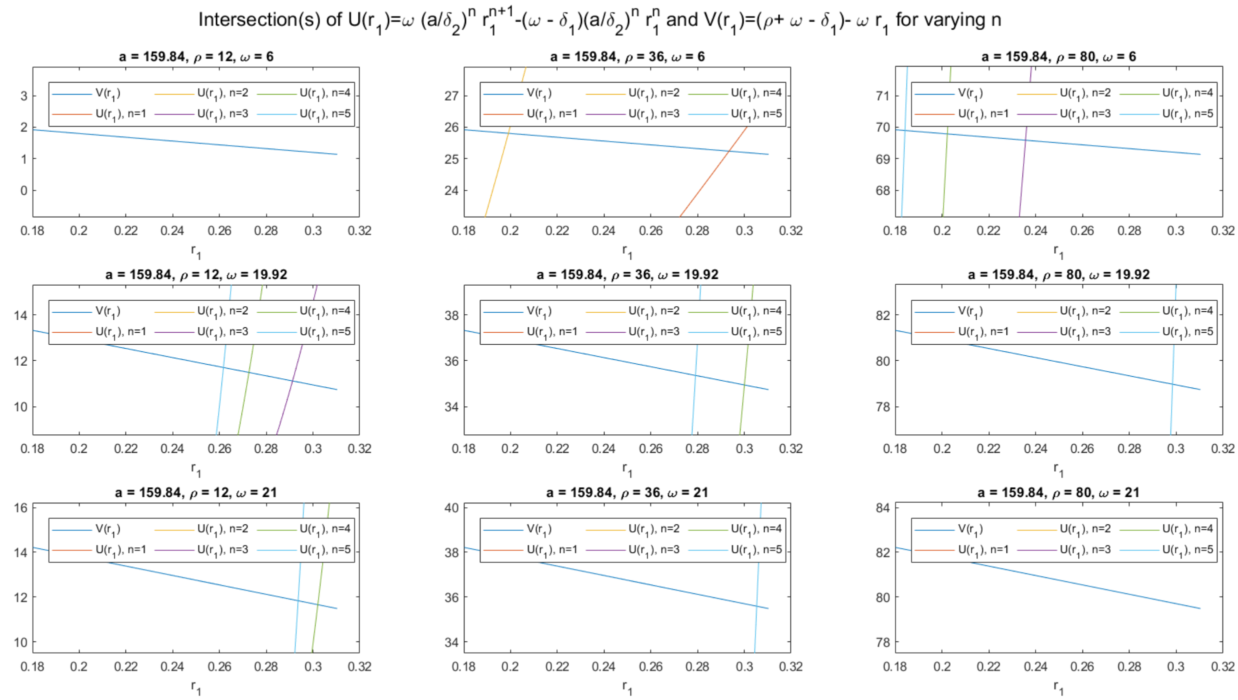

545

Figure 3.3: Graphs showing the intersection points of U and V for varying human parameter values of n, ω, and ρ with a constant to demonstrate the existence of r_1^* for case 4: hill-type f, logistic g.

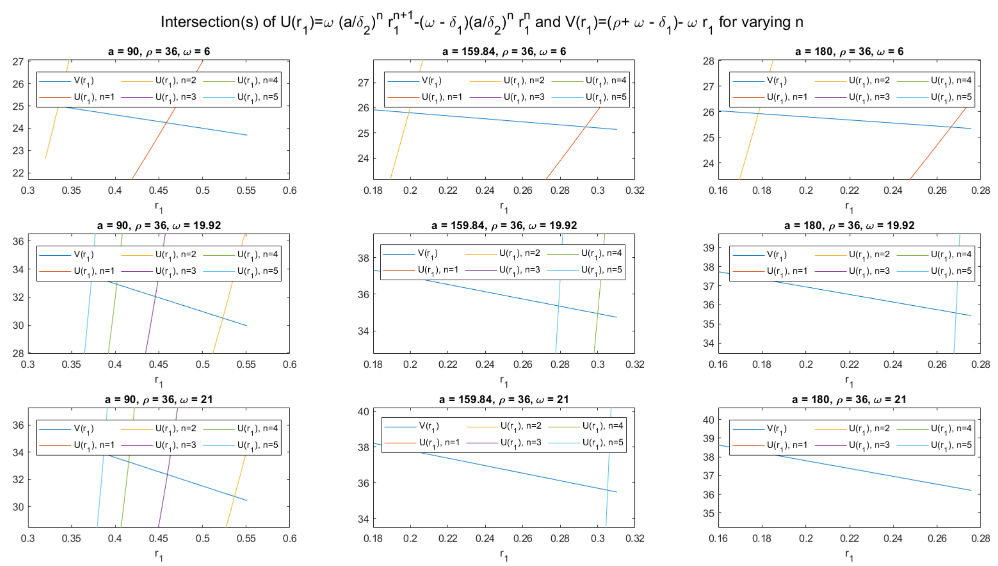

Figure 3.4: Graphs showing the intersection points of U and V for varying human parameter values of n, a, and ω with ρ constant to demonstrate the existence of r_1^* for case 4: hill-type f, logistic g.

3.4 Stability of Steady States when $H = 0$

For each of the below cases, we seek to find the stability of the nontrivial steady state values $\vec{r}^* = (r_1^*, r_2^*, r_3^*)$ determined in Chapter 3.3 of the nondimensionalized system (3.15). Much of our stability analysis can be done through examination of the Jacobian matrix and the characteristic polynomial of the nondimensionalized system (3.15). The Jacobian matrix is presented in (3.33) while the characteristic polynomial is given in (3.34).

$$J(r_1, r_2, r_3) = \begin{bmatrix} g'(r_1) - \delta_1 + \rho f(r_3) & 0 & \rho f'(r_3) r_1 \\ 1 & -\delta_2 & 0 \\ 0 & a & -1 - h'(r_3) \end{bmatrix} \tag{3.33}$$

$$p(\lambda) = -a\rho f'(r_3^*) r_1^* - (\delta_2 + \lambda)(1 + h'(r_3^*) + \lambda)(g'(r_1^*) - \delta_1 + \rho f(r_3^*) - \lambda) \tag{3.34}$$

We rewrite (3.34) in the form given in (3.35), where P, Q, and R give the coefficients of the nondimensional characteristic polynomial.

$$\begin{aligned} &\lambda^3 + P\lambda^2 + Q\lambda + R \\ &P = (1 + h'(r_3^*) + \delta_2 - g'(r_1^*) + \delta_1 - \rho f(r_3^*)) \\ &Q = (\delta_2(1 + h'(r_3^*)) + (\delta_2 + 1 + h'(r_3^*))(-g'(r_1^*) + \delta_1 - \rho f(r_3^*))) \\ &R = (-a\rho f'(r_3^*) r_1^* + \delta_2(1 + h'(r_3^*))(-g'(r_1^*) + \delta_1 - \rho f(r_3^*))) \end{aligned} \tag{3.35}$$

If the coefficients P, Q, and R satisfy the Routh-Hurwitz Criterion (2) for a specific choice of f, g, and h at a specific steady state $\vec{r}^*$, then $\vec{r}^*$ is a stable equilibrium point of the nondimensional system (3.15).

Alternatively, if there is a trivial equilibrium point $\vec{r}^* = (0, 0, 0)$, as seen in chapters 3.3.3 and 3.3.4, we may simply use the nondimensional Jacobian matrix (3.33) to determine stability. When $\vec{r}^* = \mathbf{0}$, J is the lower triangular matrix given in (3.36), hence its eigenvalues are just its diagonal entries. If all these diagonal entries are negative, the origin will be a stable steady state, otherwise it will be unstable.

$$J(0, 0, 0) = \begin{bmatrix} g'(0) - \delta_1 + \rho & 0 & 0 \\ 1 & -\delta_2 & 0 \\ 0 & a & -1 - h'(0) \end{bmatrix} \tag{3.36}$$

For each of the cases below we utilize analytic techniques or MATLAB to determine the sign of P, Q, and R and if $PQ > R$ for the nontrivial equilibrium points found in Chapter 3.3 for varying human parameter choices within the ranges given in Table 3.1 to learn more about the stability of that point. Results for mice follow analogously. For use in our model, stable equilibrium points are the most important. The stability of these points will also play into later bifurcation analysis.

3.4.1 Stability of Case 1: Linear F, Constant G

In this case we have $f(r_3) = 1 - r_3$ and $g(r_1) = 1$. From Chapter 3.3.1, we recall that ${r_3}^* = \frac{\rho - \delta_1 + \sqrt{(\rho-\delta_1)^2 + 4\rho\frac{a}{\delta_2}}}{2\rho}$ and $r_1^* = \frac{\delta_2}{a} r_3^*$. For all positive parameter choices, r_1^* and r_3^* are positive. Substitution into (3.35) yields:

$$
\begin{aligned}
P &= (1 + \delta_2 + \delta_1 - \rho + \rho r_3^*)\\
Q &= (\delta_2 + (\delta_2 + 1)(\delta_1 - \rho + \rho r_3^*))\\
R &= (a\rho r_1^* + \delta_2(\delta_1 - \rho + \rho r_3^*))
\end{aligned}
\tag{3.37}
$$

Notice that $\delta_1 - \rho + \rho r_3^* = \delta_1 - \rho + \frac{\rho-\delta_1+\sqrt{(\rho-\delta_1)^2+4\rho\frac{a}{\delta_2}}}{2} = \frac{\delta_1-\rho}{2} + \frac{\sqrt{(\delta_1-\rho)^2+4\rho\frac{a}{\delta_2}}}{2} > 0$ since $\sqrt{(\delta_1-\rho)^2 + 4\rho\frac{a}{\delta_2}} > |\delta_1 - \rho|$ as the parameters are positive. Therefore P, Q, and R are all strictly positive for relevant parameter choices. For $PQ > R$, we consult MATLAB and see that this condition holds for all parameter values given by Table 3.1. See the code given in the Appendix. Therefore the equilibrium point computed in Chapter 3.3.1 is a stable steady state for all relevant parameter values as the Routh-Hurwitz Criterion are satisfied.

In figures 3.5, 3.6, and 3.7 we generate plots of the expressions for P, Q, and R given in (3.37) in MATLAB for varying values of the parameters δ_1, δ_2, ρ, and a. We notice that, in these figures, increasing δ_2 increases the distance from the 0 plane, while changing δ_1 impacts the asymptotic behavior for small values of ρ.

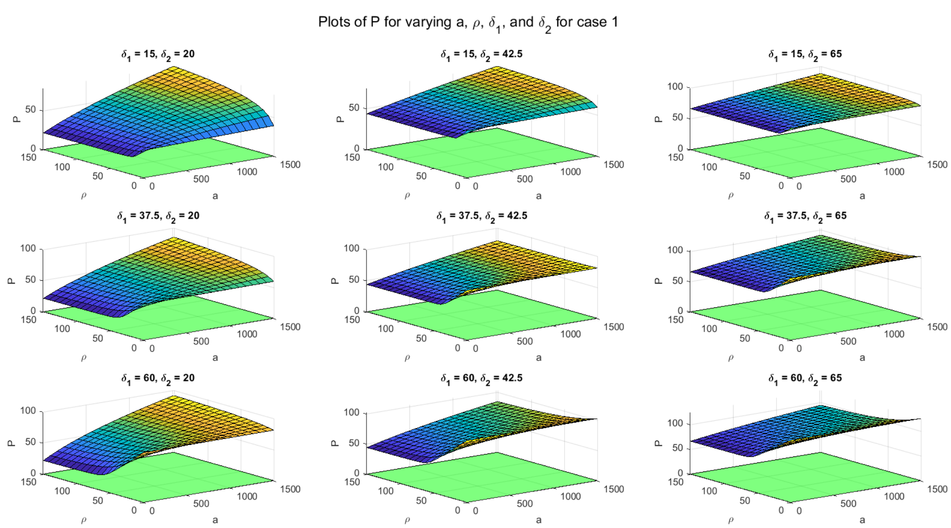

Figure 3.5: For case 1: linear f, constant g, the surface P is plotted as a function of varying δ_1, δ_2, ρ, and a. For all values, the surface P lies above the green plane representing $P = 0$.

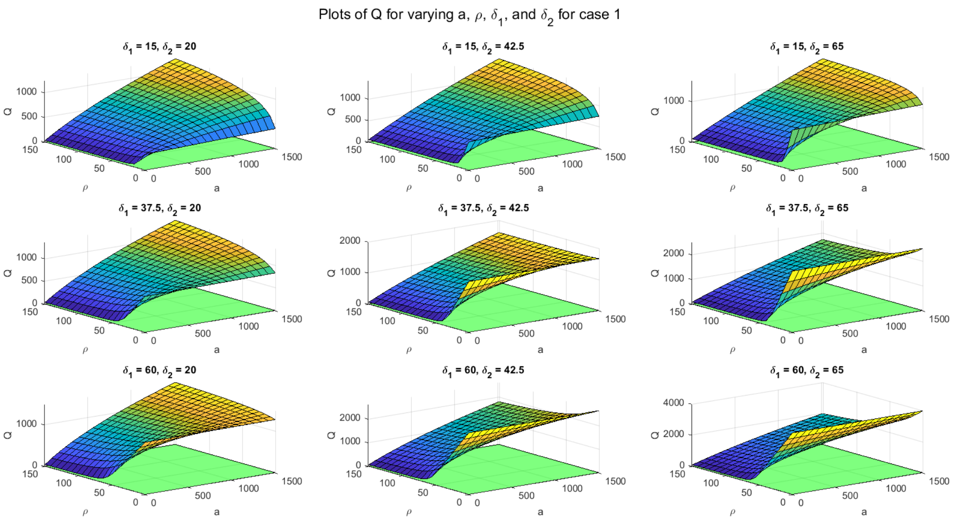

Figure 3.6: For case 1: linear f, constant g, the surface Q is plotted as a function of varying δ_1, δ_2, ρ, and a. For all values, the surface Q lies above the green plane representing $Q = 0$.

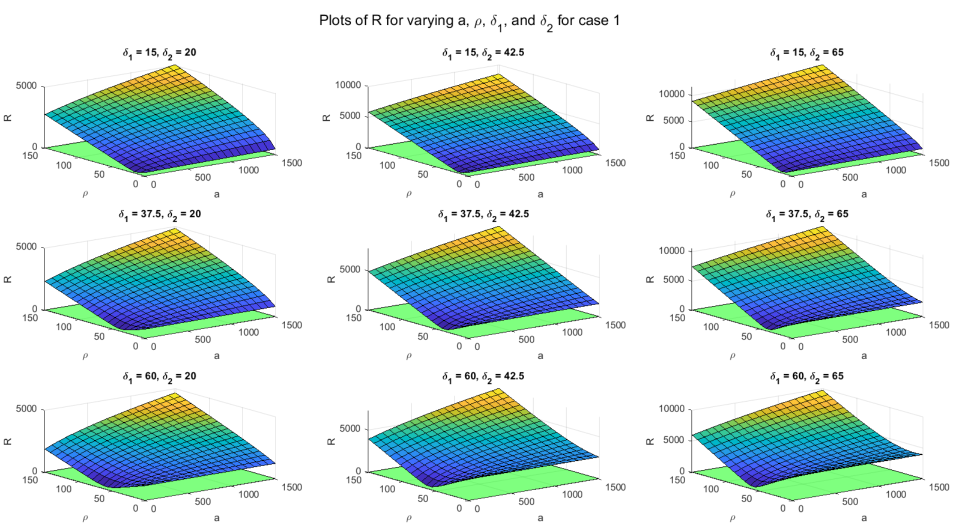

Figure 3.7: For case 1: linear f, constant g, the surface R is plotted as a function of varying δ_1, δ_2, ρ, and a. For all values, the surface R lies above the green plane representing $R = 0$.

3.4.2 Stability of Case 2: Hill-type F, Constant G

In this case we have $f(r_3) = \frac{1}{1+r_3^n}$ and $g(r_1) = 1$. Substitution into (3.35) yields:

$$
\begin{aligned}
P &= (1 + \delta_2 + \delta_1 - \rho\frac{1}{1 + r_3^{*n}}) \\
Q &= (\delta_2 + (\delta_2 + 1)(\delta_1 - \rho\frac{1}{1 + r_3^{*n}})) \\
R &= (a\rho\frac{n r_3^{*n-1}}{(r_3^{*n} + 1)^2} r_1^* + \delta_2(\delta_1 - \rho\frac{1}{1 + r_3^{*n}}))
\end{aligned}
\tag{3.38}
$$

We generate plots of the expressions for P, Q, and R given in (3.38) in MATLAB for varying values of the parameters δ_1, δ_2, ρ, and a to determine the signs of these values. From figures 3.8, 3.9, and 3.10, we see that P, Q, and R are all strictly positive for relevant parameter choices. This means that the characteristic polynomial for this case has no positive real roots. However, to determine the stability of the equilibrium point computed in Chapter 3.3.2, we also must examine the inequality $PQ > R$. In Figure 3.11 we plot PQ/R for varying values of the parameters δ_1, δ_2, ρ, and a. If the surface PQ/R lies in the range [0,1], we have $PQ < R$ and hence the Routh-Hurwitz Criterion are not satisfied. We notice that for small values of δ_1 and large values of ρ, the surface falls into this range. Therefore, choice of parameters with the ranges given by Table 3.1 can drive the equilibrium away from being stable. From figures 3.8, 3.9, and 3.10, we note that, like the previous case, in these figures, increasing δ_2 increases the distance from the 0 plane, while changing δ_1 impacts the asymptotic behavior for small values of ρ.

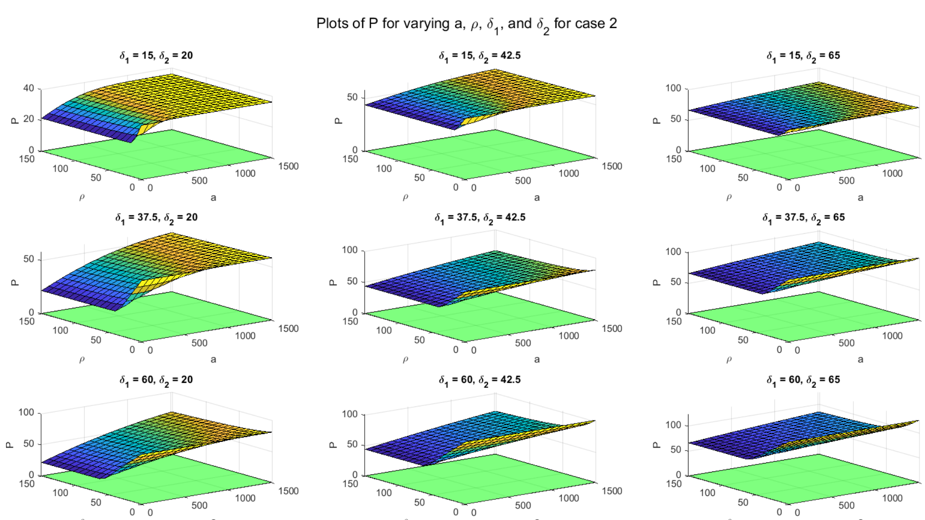

Figure 3.8: For case 2: hill-type f, constant g, the surface P is plotted as a function of varying δ_1, δ_2, ρ, and a. For all values, the surface P lies above the green plane representing $P = 0$.

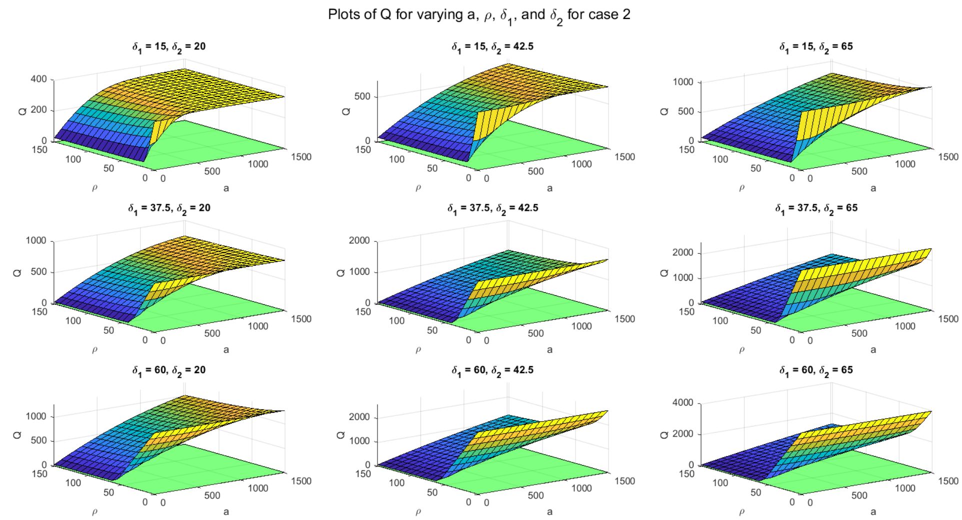

Figure 3.9: For case 2: hill-type f, constant g, the surface Q is plotted as a function of varying δ_1, δ_2, ρ, and a. For all values, the surface Q lies above the green plane representing $Q = 0$.

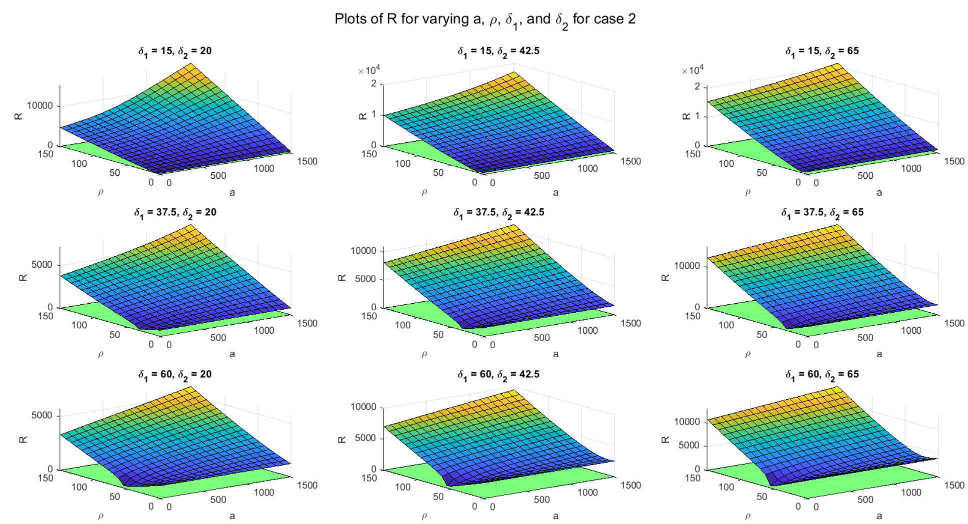

Figure 3.10: For case 2: hill-type f, constant g, the surface R is plotted as a function of varying δ_1, δ_2, ρ, and a. For all values, the surface R lies above the green plane representing $R = 0$.

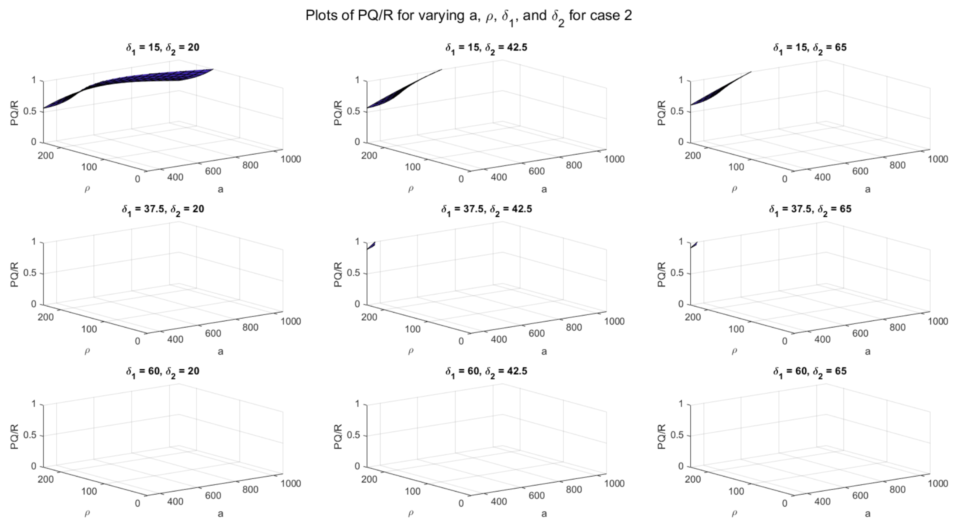

Figure 3.11: For case 2: hill-type f, constant g, the surface PQ/R is plotted as a function of varying δ_1, δ_2, ρ, and a. We restrict the z-axis range to [0,1]. For some parameter values (first row), larger values of ρ cause the surface to be within this range, indicating that $PQ < R$, so the corresponding equilibrium point is not stable.

3.4.3 Stability of Case 3: Linear F, Logistic G

In this case we have $f(r_3) = 1 - r_3$ and $g(r_1) = \omega r_1(1 - r_1)$. We represent the nontrivial equilibrium point by $\vec{r}^* = (r_1^*, r_2^*, r_3^*)$ and recall that $r_1^* = \frac{\rho-\delta_1+\omega}{\omega+\rho\frac{a}{\delta_2}}$ and $r_3^* = \frac{a}{\delta_2} r_1^*$ with existence only when $(\rho - \delta_1 + \omega) > 0$. Substitution into (3.35) yields:

$$\begin{aligned} P &= (1 + \delta_2 + 2\omega r_1^* - \omega + \delta_1 - \rho + \rho r_3^*) \\ Q &= (\delta_2 + (\delta_2 + 1)(2\omega r_1^* - \omega + \delta_1 - \rho + \rho r_3^*)) \\ R &= (a\rho r_1^* + \delta_2(2\omega r_1^* - \omega + \delta_1 - \rho + \rho r_3^*)) \end{aligned} \tag{3.39}$$

Notice that $2\omega r_1^* - \omega + \delta_1 - \rho + \rho r_3^* = -(\rho - \delta_1 + \omega) + 2\omega r_1^* + \rho\frac{a}{\delta_2} r_1^* = -(\rho - \delta_1 + \omega) + (2\omega + \rho\frac{a}{\delta_2})r_1^* = -r_1^*(\omega + \rho\frac{a}{\delta_2}) + (2\omega + \rho\frac{a}{\delta_2})r_1^* = \omega r_1^*$. Therefore, P, Q, and R may be simplified considerably to (3.40).

$$\begin{aligned} P &= 1 + \delta_2 + \omega r_1^* \\ Q &= \delta_2 + (\delta_2 + 1)\omega r_1^* \\ R &= a\rho r_1^* + \delta_2 \omega r_1^* \end{aligned} \tag{3.40}$$

As we required $(\rho - \delta_1 + \omega) > 0$ and positive parameter values for the existence of r_1^* and r_3^*, it follows that $r_1^* > 0$ and $r_3^* > 0$. Therefore P, Q, and R are all strictly positive for relevant parameter choices. For $PQ > R$, we observe the plot of PQ/R for varying values of the parameters δ_1, δ_2, ρ, and ω given in Figure 3.12. If the surface PQ/R lies in the range [0,1], we have $PQ < R$ and hence the Routh-Hurwitz Criterion are not satisfied. We notice that for small values of δ_1 and δ_2 and large values of ρ, the surface falls into this range. Therefore, choice of parameters with the ranges given by Table 3.1 can drive the nontrivial equilibrium point computed in Chapter 3.3.3 away from being stable.

In figures 3.13, 3.14, and 3.15, we generate plots of the expressions for P, Q, and R given in (3.39) in MATLAB for varying values of the parameters δ_1, δ_2, ρ, and ω. We also plot the condition $(\rho - \delta_1 + \omega) > 0$ to make clear which parameter choices result in a viable equilibrium point. We note that, like in the preceding cases, in these figures, increasing δ_2 increases the distance from the 0 plane, while changing δ_1 impacts the asymptotic behavior for small values of ρ.

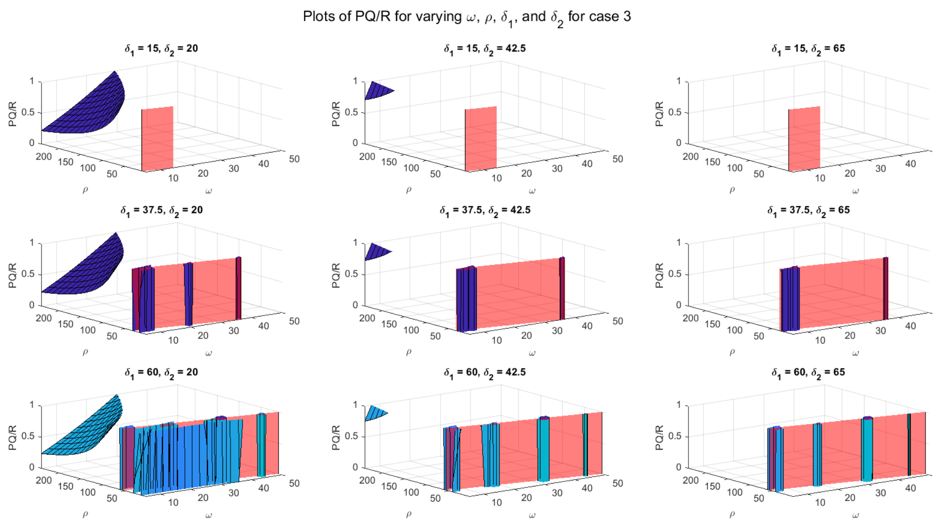

Figure 3.12: For case 3: linear f, logistic g, the surface PQ/R is plotted as a function of varying δ_1, δ_2, ρ, and ω for $a = 79.98$. The condition for existence given in Chapter 3.3.3, $(\rho - \delta_1 + \omega) > 0$, is represented by the portion of the surface lying behind the red plane. We restrict the z-axis range to [0,1]. For some parameter values (first two columns), larger values of ρ cause the surface to be within this range, indicating that $PQ < R$, so the corresponding equilibrium point is not stable. Values plotted along the plane $(\rho - \delta_1 + \omega) = 0$ are asymptotic and do not contribute to our analysis.

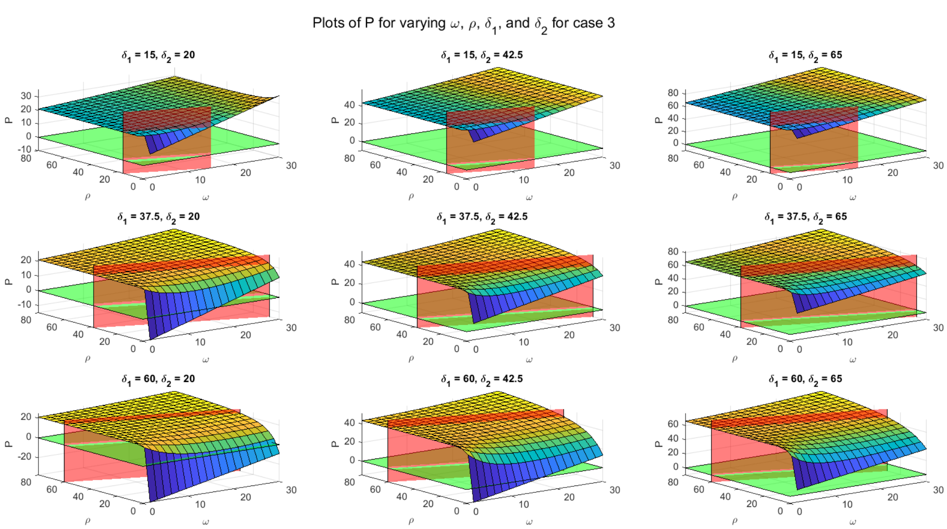

Figure 3.13: For case 3: linear f, logistic g, the surface P is plotted as a function of varying δ_1, δ_2, ρ, and ω for $a = 79.98$. For all values satisfying the condition for existence given in Chapter 3.3.3, $(\rho - \delta_1 + \omega) > 0$, given by the portion of the surface lying behind the red plane, the surface P lies above the green plane representing $P = 0$.

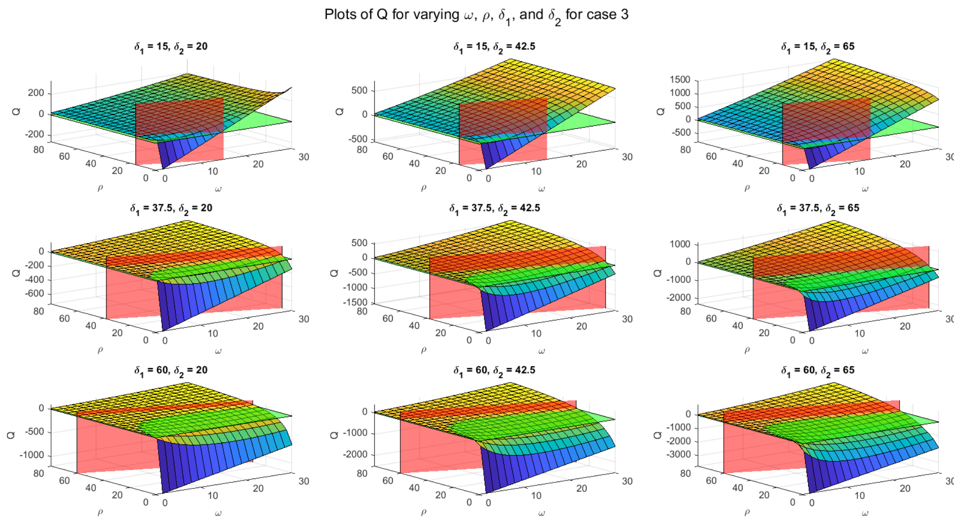

Figure 3.14: For case 3: linear f, logistic g, the surface Q is plotted as a function of varying δ_1, δ_2, ρ, and ω for $a = 79.98$. For all values satisfying the condition for existence given in Chapter 3.3.3, $(\rho - \delta_1 + \omega) > 0$, given by the portion of the surface lying behind the red plane, the surface Q lies above the green plane representing $Q = 0$.

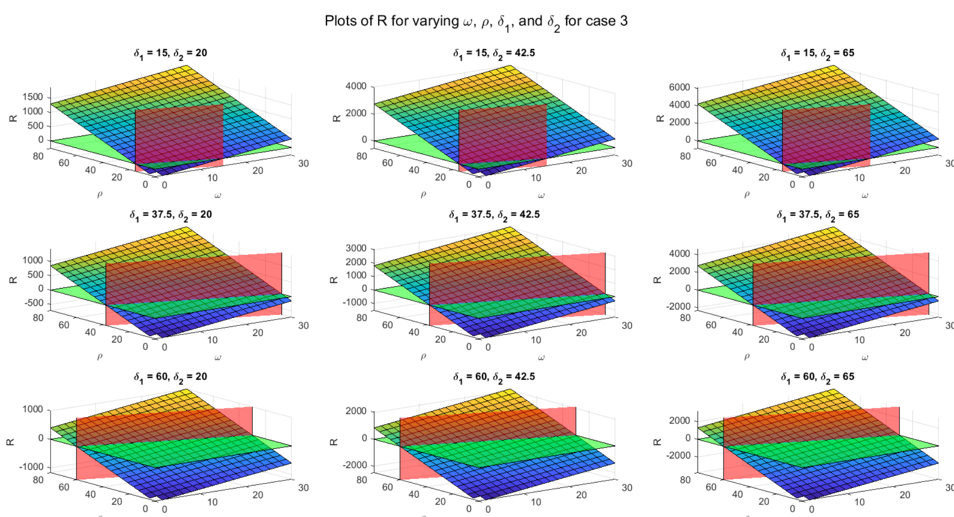

645

Figure 3.15: For case 3: linear f, logistic g, the surface R is plotted as a function of varying δ_1, δ_2, ρ, and ω for $a = 79.98$. For all values satisfying the condition for existence given in Chapter 3.3.3, $(\rho - \delta_1 + \omega) > 0$, given by the portion of the surface lying behind the red plane, the surface R lies above the green plane representing $R = 0$.

For the trivial steady state, on the other hand, we calculate the nondimensional Jacobian from (3.36).

$$J(0,0,0) = \begin{bmatrix} \omega - 2\omega(0) - \delta_1 + \rho & 0 & 0 \\ 1 & -\delta_2 & 0 \\ 0 & a & -1 \end{bmatrix} = \begin{bmatrix} \omega - \delta_1 + \rho & 0 & 0 \\ 1 & -\delta_2 & 0 \\ 0 & a & -1 \end{bmatrix} \tag{3.41}$$

From (3.41), we see that all eigenvalues of $J(0,0,0)$ are negative (corresponding to a stable steady state at the origin) when $(\rho - \delta_1 + \omega) < 0$, otherwise the origin is not stable. This makes sense, as the nontrivial positive equilibrium point only exists for $(\rho - \delta_1 + \omega) > 0$, and we saw above that it is always stable in that case.

3.4.4 Stability of Case 4: Hill-type F, Logistic G

In this case we have $f(r_3) = \frac{1}{1+r_3^n}$ and $g(r_1) = \omega r_1(1 - r_1)$. Substitution into (3.35), where $\vec{r}^* = (r_1^*, r_2^*, r_3^*)$ represents the nontrivial equilibrium point, yields:

$$\begin{aligned} P &= (1 + \delta_2 + 2\omega r_1^* - \omega + \delta_1 - \rho\frac{1}{1 + r_3^{*n}}) \\ Q &= (\delta_2 + (\delta_2 + 1)(2\omega r_1^* - \omega + \delta_1 - \rho\frac{1}{1 + r_3^{*n}})) \\ R &= (a\rho\frac{n r_3^{*n-1}}{(r_3^{*n} + 1)^2} r_1^* + \delta_2(2\omega r_1^* - \omega + \delta_1 - \rho\frac{1}{1 + r_3^{*n}})) \end{aligned} \tag{3.42}$$

We generate plots of the expressions for P, Q, and R given in (3.42) in MATLAB for varying values of the parameters δ_1, δ_2, ρ, and a with $\omega = 19.92$ to determine the signs of these values. From figures 3.17, 3.18, and 3.19, we see that P, Q, and R are all strictly positive for relevant parameter choices. This means that the characteristic polynomial for this case has no positive real roots. However, to determine the stability of the equilibrium point computed in Chapter 3.3.4, we also must examine the inequality $PQ > R$. In Figure 3.16 we plot PQ/R. If the surface PQ/R lies in the range [0,1], we have $PQ < R$ and hence the Routh-Hurwitz Criterion are not satisfied. We notice that for small values of δ_2 and large values of ρ, the surface falls into this range. Therefore, choice of parameters with the ranges given by Table 3.1 can drive the equilibrium away from being stable.

From figures 3.17, 3.18, and 3.19, we note that, like in the preceding three cases, increasing δ_2 increases the distance from the 0 plane, while changing δ_1 impacts the asymptotic behavior for small values of ρ. However, unlike the previous cases, in regions where the condition $\delta_1 \geq (\rho + \omega)$ given by Theorem 3.3.4 is satisfied, there is no steady state value and consequently no P, Q, or R surface to be plotted for the corresponding parameter values.

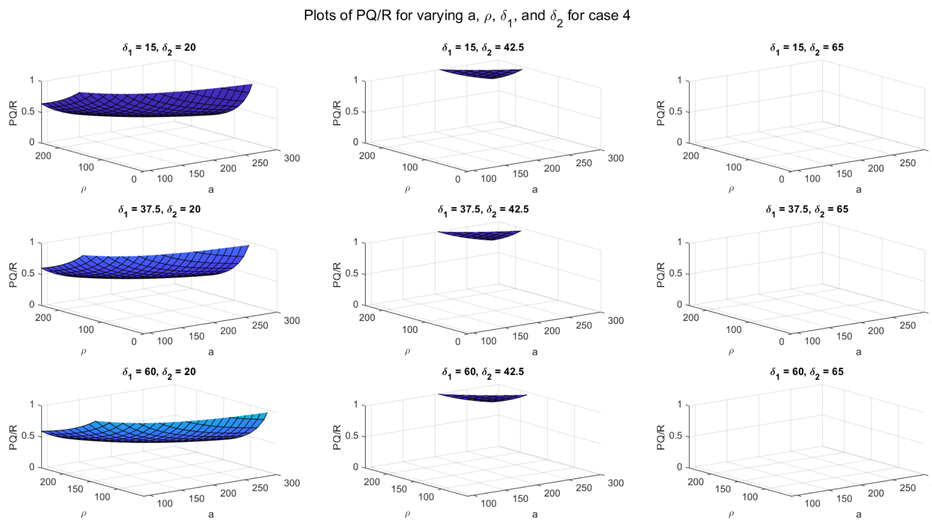

Figure 3.16: For case 4: hill-type f, logistic g, the surface PQ/R is plotted as a function of varying δ_1, δ_2, ρ, and a for $\omega = 19.92$. We restrict the z-axis range to [0,1]. For some parameter values (first two columns), larger values of ρ cause the surface to be within this range, indicating that $PQ < R$, so the corresponding equilibrium point is not stable.

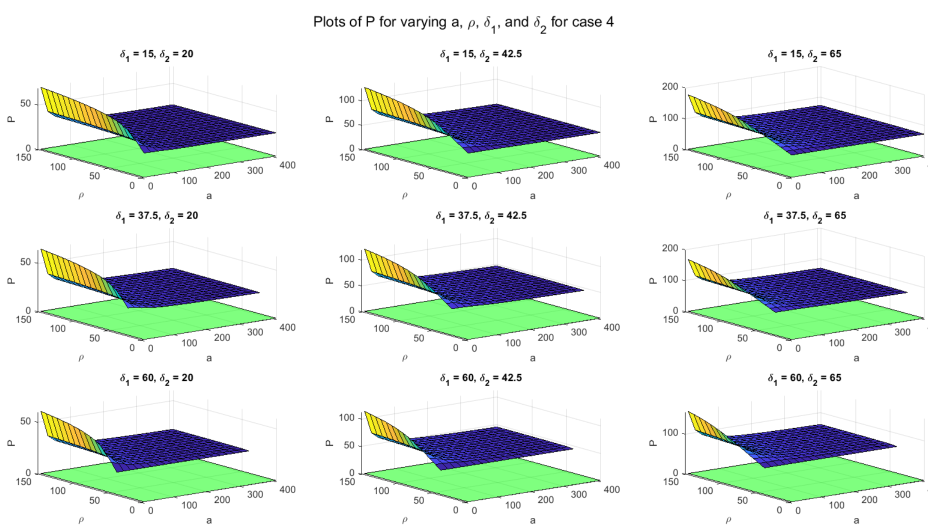

Figure 3.17: For case 4: hill-type f, logistic g, the surface P is plotted as a function of varying δ_1, δ_2, ρ, and a for $\omega = 19.92$. For all values, the surface P lies above the green plane representing $P = 0$.

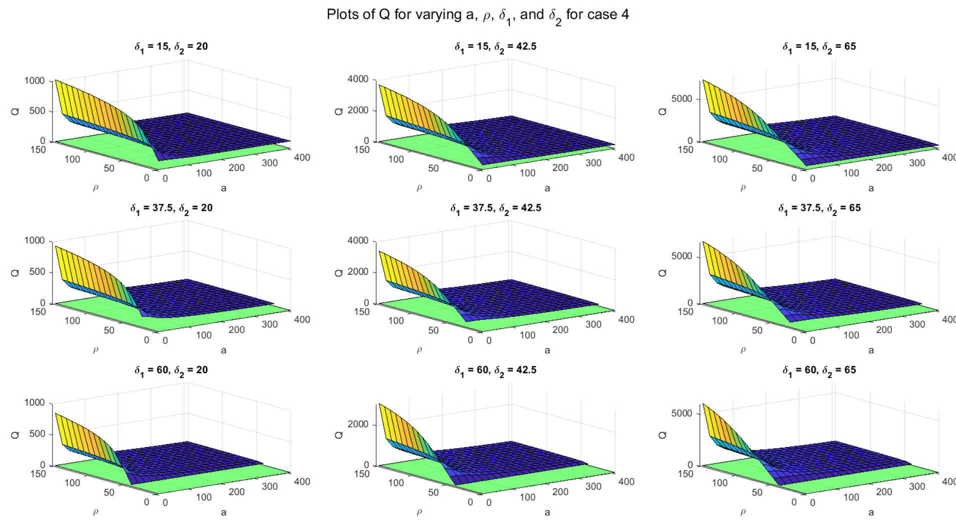

Figure 3.18: For case 4: hill-type f, logistic g, the surface Q is plotted as a function of varying δ_1, δ_2, ρ, and a for $\omega = 19.92$. For all values, the surface Q lies above the green plane representing $Q = 0$.

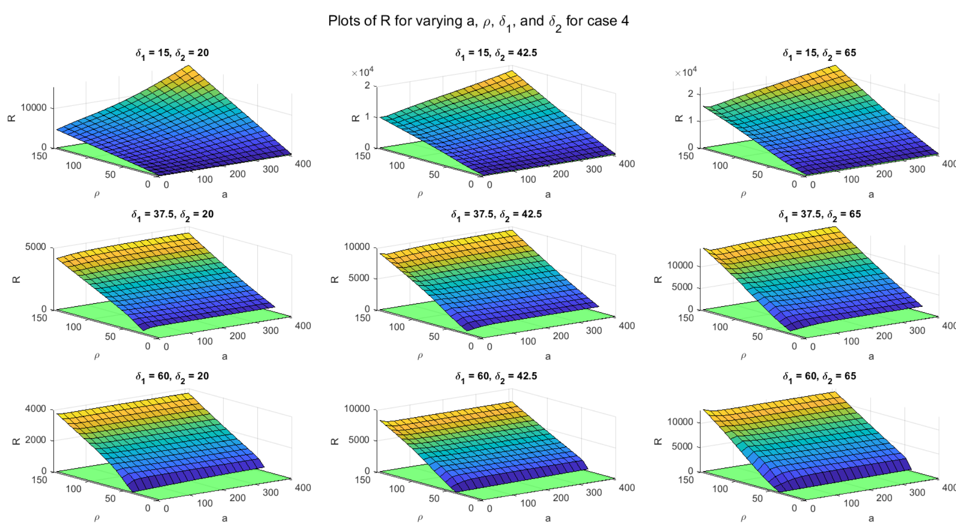

Figure 3.19: For case 4: hill-type f, logistic g, the surface R is plotted as a function of varying δ_1, δ_2, ρ, and a for $\omega = 19.92$. For all values, the surface R lies above the green plane representing $R = 0$.

For the trivial steady state, on the other hand, we calculate the nondimensional Jacobian from (3.33) in (3.43).

$$J(0,0,0) = \begin{bmatrix} \omega - 2\omega(0) - \delta_1 + \rho\frac{1}{1+0^n} & 0 & 0 \\ 1 & -\delta_2 & 0 \\ 0 & a & -1 \end{bmatrix} = \begin{bmatrix} \omega - \delta_1 + \rho & 0 & 0 \\ 1 & -\delta_2 & 0 \\ 0 & a & -1 \end{bmatrix} \tag{3.43}$$

From (3.41), we see that all eigenvalues of $J(0,0,0)$ are negative (corresponding to a stable steady state at the origin) when $(\rho - \delta_1 + \omega) < 0$, otherwise the origin is unstable.

3.5 Bifurcation Analysis when $H = 0$

Theorem 10. *If the characteristic polynomial, written $\lambda^3 + P\lambda^2 + Q\lambda + R = 0$, of a system of ordinary differential equations has the property that $R = PQ$ for some value $\vec{R}_h$ in the system, then the system exhibits a Hopf Bifurcation at $\vec{R}_h$.*

Proof. See Ngonghala et al. [12]. □

Theorem 11. *The initial amplitude of solutions of (2.1) at the Hopf Bifurcation point $\vec{R}_h$, should it exist, is given by* $\exp(\frac{PQ\varepsilon\upsilon\tau}{2(Q+P^2)})$.

Proof. We use the methodology of Ngwa [13]. Let $\xi = \frac{R}{PQ} > 0$, where P, Q, and R are defined in Proposition 4. By theorem 12, at $\xi = \xi_c = 1$ (2.1) undergoes a Hopf Bifurcation. Write $\lambda = \lambda(\xi)$, such that the roots of the characteristic polynomial are defined as a continuous function of ξ. Thus the characteristic polynomial given in Proposition 4 may be written as:

$$\lambda^3(\xi) + P\lambda^2(\xi) + Q\lambda(\xi) + \xi PQ = 0 \tag{3.44}$$

At ξ_c, (3.44) has a purely imaginary solution pair of $\lambda(\xi_c) = \pm i\sqrt{Q}$ and a negative real solution of $\lambda(\xi_c) = -P$. Implicitly differentiating (3.44) at $\xi = \xi_c$ and substituting the imaginary solution pair yields:

$$\lambda'(\xi_c) = \frac{-PQ}{3\lambda^2(\xi_c) + 2P\lambda(\xi_c) + Q} = \frac{P(Q \pm P\sqrt{Q}i)}{2(Q+P^2)} \tag{3.45}$$

For $0 < \varepsilon << 1$ and $\upsilon = \pm 1$, a small perturbation away from the Hopf bifurcation ξ_c can be represented as $\xi_c + \varepsilon\upsilon$. By Taylor Expansion and substitution of (3.45):

$$\lambda(\xi_c + \varepsilon\upsilon) \approx \lambda(\xi_c) + \lambda'(\xi_c)\varepsilon\upsilon = \frac{PQ}{2(Q+P^2)}\varepsilon\upsilon \pm i\sqrt{Q}(1 + \frac{P^2}{2(Q+P^2)}\varepsilon\upsilon) \tag{3.46}$$

Thus, oscillatory solutions at ξ_c have initial amplitude given by:

$$\exp(\frac{PQ\varepsilon\upsilon\tau}{2(Q+P^2)}) \tag{3.47}$$

Depending on the value of υ, the amplitude will either grow ($\upsilon = 1$), or decay to zero ($\upsilon = -1$). □

For cases 1 (3.3.1) and 3 (3.3.3), where we obtained a closed form expression for $\vec{r}^*$, we seek to find relationships among the parameters to describe the Hopf bifurcation given when $PQ = R$ or $PQ - R = 0$ as described by Theorem 10 for the steady states determined in Chapter 3.3. We explain equations for the bifurcation lotus as functions of the nondimensional parameters.

For case 1, we recall that $r_1^* = \dfrac{\rho - \delta_1 + \sqrt{(\rho-\delta_1)^2 + 4\rho\frac{a}{\delta_2}}}{2\rho\frac{a}{\delta_2}}$ and $r_3^* = \frac{a}{\delta_2} r_1^*$, with P, Q, and R given by (3.37). To simplify notation, let $A = (1+\delta_2)$ and $B = \rho - \delta_1$. Then we have the following:

$$P = A - B + \rho\frac{a}{\delta_2}r_1^*; \quad Q = \delta_2 + A\left(-B + \rho\frac{a}{\delta_2}r_1^*\right); \quad R = a\rho r_1^* + \delta_2 + \delta_2\left(-B + \rho\frac{a}{\delta_2}r_1^*\right)$$

$$r_1^* = \frac{\rho - \delta_1 + \sqrt{(\rho-\delta_1)^2 + 4\rho\frac{a}{\delta_2}}}{2\rho\frac{a}{\delta_2}} \Rightarrow \rho\frac{a}{\delta_2}r_1^* = \frac{B + \sqrt{B^2 + 4\rho\frac{a}{\delta_2}}}{2}$$

Thus we have:

$$\begin{aligned}
P &= A - B + \frac{B + \sqrt{B^2 + 4\rho\frac{a}{\delta_2}}}{2} = A - \frac{B}{2} + \frac{\sqrt{B^2 + 4\rho\frac{a}{\delta_2}}}{2}\\
Q &= \delta_2 + A\left(-B + \frac{B + \sqrt{B^2 + 4\rho\frac{a}{\delta_2}}}{2}\right) = \delta_2 + A\left(-\frac{B}{2} + \frac{\sqrt{B^2 + 4\rho\frac{a}{\delta_2}}}{2}\right);\\
R &= a\rho r_1^* + \delta_2 + \delta_2\left(-B + \frac{B + \sqrt{B^2 + 4\rho\frac{a}{\delta_2}}}{2}\right)\\
&= \delta_2\left(\frac{B + \sqrt{B^2 + 4\rho\frac{a}{\delta_2}}}{2}\right) + \delta_2 + \delta_2\left(-\frac{B}{2} + \frac{\sqrt{B^2 + 4\rho\frac{a}{\delta_2}}}{2}\right)\\
&= \delta_2\left(\sqrt{B^2 + 4\rho\frac{a}{\delta_2}}\right) + \delta_2 = \delta_2\left(1 + \sqrt{B^2 + 4\rho\frac{a}{\delta_2}}\right)
\end{aligned}$$

$$\begin{aligned}
PQ &= \left(A - \frac{B}{2} + \frac{\sqrt{B^2 + 4\rho\frac{a}{\delta_2}}}{2}\right)\left(\delta_2 + A\left(-\frac{B}{2} + \frac{\sqrt{B^2 + 4\rho\frac{a}{\delta_2}}}{2}\right)\right)\\
&= \left(A - \frac{B}{2}\right)\left(\delta_2 - A\frac{B}{2}\right) + \frac{\sqrt{B^2 + 4\rho\frac{a}{\delta_2}}}{2}A\left(A - \frac{B}{2} + \delta_2 - A\frac{B}{2}\right) + \frac{A}{4}\left(B^2 + 4\rho\frac{a}{\delta_2}\right)\\
&= A\delta_2 + \frac{A}{2}B^2 - \left(A^2 + \delta_2\right)\frac{B}{2} + A\rho\frac{a}{\delta_2} + \frac{\sqrt{B^2 + 4\rho\frac{a}{\delta_2}}}{2}A\left(A - \frac{B}{2} + \delta_2 - A\frac{B}{2}\right)
\end{aligned}$$

Then setting $PQ = R$ implies that:

$$
\begin{aligned}
&A\delta_2 + \frac{A}{2}B^2 - \left(A^2+\delta_2\right)\frac{B}{2} + A\rho\frac{a}{\delta_2} + \frac{\sqrt{B^2+4\rho\frac{a}{\delta_2}}}{2}A\left(A - \frac{B}{2} + \delta_2 - A\frac{B}{2}\right) \\
&= \delta_2\left(1 + \sqrt{B^2+4\rho\frac{a}{\delta_2}}\right) \\
\Longrightarrow\ &A\delta_2 + \frac{A}{2}B^2 - \left(A^2+\delta_2\right)\frac{B}{2} + A\rho\frac{a}{\delta_2} - \delta_2 \\
&= \delta_2\sqrt{B^2+4\rho\frac{a}{\delta_2}} - \frac{\sqrt{B^2+4\rho\frac{a}{\delta_2}}}{2}A\left(A - \frac{B}{2} + \delta_2 - A\frac{B}{2}\right)
\end{aligned}
$$

Letting $\Gamma = \delta_2 - \frac{1}{2}A\left(1+2\delta_2\right)$, we can rewrite and further simplify the left-hand-side (LHS) and right-hand-side (RHS) of the expression above.

$$
\begin{aligned}
LHS &= A\delta_2 + \frac{A}{2}B^2 - \left(A^2+\delta_2\right)\frac{B}{2} + A\rho\frac{a}{\delta_2} - \delta_2 \\
&= \delta_2^2 + \frac{A}{2}B^2 - \left(A^2+\delta_2\right)\frac{B}{2} + A\rho\frac{a}{\delta_2} \\
RHS &= \sqrt{B^2+4\rho\frac{a}{\delta_2}}\left(\delta_2 - \frac{1}{2}A\left(A - \frac{B}{2} + \delta_2 - A\frac{B}{2}\right)\right) \\
&= \sqrt{B^2+4\rho\frac{a}{\delta_2}}\left(\delta_2 - \frac{1}{2}A\left(1+2\delta_2\right) + \frac{AB}{4}\left(2+\delta_2\right)\right) \\
&= \left(\Gamma + \frac{AB}{4}\left(2+\delta_2\right)\right)\sqrt{B^2+4\rho\frac{a}{\delta_2}}
\end{aligned}
$$

Therefore:

$$
LHS = RHS \implies \delta_2^2 + \frac{A}{2}B^2 - \left(A^2+\delta_2\right)\frac{B}{2} + A\rho\frac{a}{\delta_2} = \left(\Gamma + \frac{AB}{4}\left(2+\delta_2\right)\right)\sqrt{B^2+4\rho\frac{a}{\delta_2}}
$$

Squaring both sides, we see:

$$
\begin{aligned}
&\left(\delta_2^2 + \frac{A}{2}B^2 - \left(A^2+\delta_2\right)\frac{B}{2} + A\rho\frac{a}{\delta_2}\right)^2 = \left(\Gamma + \frac{AB}{4}\left(2+\delta_2\right)\right)^2\left(B^2+4\rho\frac{a}{\delta_2}\right) \Longrightarrow \\
&\left(\delta_2^2 + \frac{A}{2}B^2 - \left(A^2+\delta_2\right)\frac{B}{2}\right)^2 + A^2\rho^2\left(\frac{a}{\delta_2}\right)^2 + 2\left(\delta_2^2 + \frac{A}{2}B^2 - \left(A^2+\delta_2\right)\frac{B}{2}\right)\left(A\rho\frac{a}{\delta_2}\right) \\
&= \left(\Gamma + \frac{AB}{4}\left(2+\delta_2\right)\right)^2 B^2 + \left(\Gamma + \frac{AB}{4}\left(2+\delta_2\right)\right)^2 4\rho\frac{a}{\delta_2}
\end{aligned}
$$

Finally, we can write this expression as a polynomial in a and use the quadratic formula to write an expression for a in terms of the other parameters to characterize the bifurcation lotus. By this methodology, the above transforms to:

$$
\begin{aligned}
&a^2 + Ma + N = 0\\
&\qquad M = \frac{\delta_2}{A\rho}\left(2\left(\delta_2^2 + \frac{A}{2}B^2 - \left(A^2+\delta_2\right)\frac{B}{2}\right) - \left(\Gamma + \frac{AB}{4}\left(2+\delta_2\right)\right)^2\right)\\
&\qquad N = \frac{\delta_2^2}{A^2\rho^2}\left[\left(\delta_2^2 + \frac{A}{2}B^2 - \left(A^2+\delta_2\right)\frac{B}{2}\right)^2 - \left(\Gamma + \frac{AB}{4}\left(2+\delta_2\right)\right)^2 B^2\right]
\end{aligned}
$$

For case 3, we recall that $r_1^* = \frac{\rho-\delta_1+\omega}{\omega+\rho\frac{a}{\delta_2}}$ and $r_3^* = \frac{a}{\delta_2}r_1^*$, with the most simplified forms P, Q, and R given by (3.40). We restate (3.40):

$$
\begin{aligned}
P &= 1 + \delta_2 + \omega r_1^*\\
Q &= \delta_2 + (\delta_2+1)\omega r_1^*\\
R &= a\rho r_1^* + \delta_2\omega r_1^*
\end{aligned}
$$

Next, notice that $R = r_1^*(a\rho + \delta_2\omega) = \delta_2 r_1^*(\omega + \rho\frac{a}{\delta_2}) = \delta_2(\rho - \delta_1 + \omega)$. Meanwhile, $PQ = \delta_2 + (\delta_2+1)\omega r_1^* + \delta_2^2 + \delta_2(\delta_2+1)\omega r_1^* + \delta_2\omega r_1^* + (\delta_2+1)\omega^2(r_1^*)^2$. To find a convenient expression for $PQ - R = 0$, we simplify the expression, yielding the expression in (3.48).

$$
(PQ - R) = \delta_2(1+\delta_2) + [(1+\delta_2)^2\omega - a\rho]r_1^* + (\delta_2+1)\omega^2(r_1^*)^2 = 0 \qquad (3.48)
$$

From (3.48) we could form polynomials in each of the parameters ρ, a, and ω by multiplying the expression by $(\omega + \rho\frac{a}{\delta_2})^2$. Then, using the quartic, cubic, and quadratic formulas would form an expression for ρ, a, and ω in terms of the other parameters to represent the bifurcation lotus. As we required $(\rho - \delta_1 + \omega) > 0$ for this steady state to exist, we can conclude the following from (3.48).

Remark 5. *For $PQ - R = 0$ in this case, it is necessary that $\omega(1+\delta_2)^2 < a\rho$.*

In figure 3.20, we display an implicit plot of the three dimensional bifurcation plot in a, ρ, ω space. For the scope of this thesis, we do not consider bifurcations in δ_1 or δ_2.

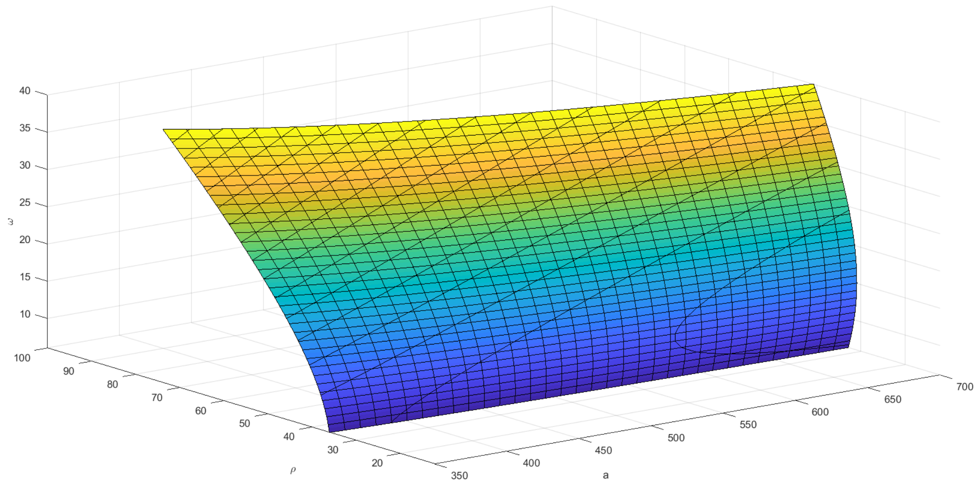

Figure 3.20: We implicitly plot the solutions to $(PQ-R) = \delta_2(1+\delta_2)+[(1+\delta_2)^2\omega - a\rho]r_1^* + (\delta_2+1)\omega^2(r_1^*)^2 = 0$ to give a bifurcation plot in a, ρ, ω space for case 3: linear f, logistic g with $\delta_1 = 15$ and $\delta_2 = 20$.

Chapter 4

Numerical Analyses for $H = 0$

We run numerical simulations of the system (2.1) in MATLAB using a modified code for plotting the Lorenz equations [6] and the numerical bifurcation package MATCONT for MATLAB, with Hil Meijer's tutorials [11]. In all cases we use the initial conditions (2.2) of $R_1^0 = 1.6653$, $R_2^0 = 1.249$, and $R_3^0 = 22.5$ to represent a small perturbation away from the theoretical equilibrium state of $R_3 = 24.98$ to allow us to better observe any transient dynamics of the system (2.1).

4.1 Analysis for Case 1: Linear F, Constant G

Here we have $F(R_3) = 1 - \frac{R_3}{s}$ and $G(R_1) = L$. In figure 4.1, we display bifurcation plots for the system, using parameter handles of γ and L, for parameter values in and around those given in table 2.5. We see the bifurcation lotus in the γ, L plane divides the space into two regions, the first of which (labeled I) corresponds to stable fixed points and the second of which (II) corresponds to stable limit cycles. This relationship is illustrated in figure 4.2. Finally, plots in $R_1 \times R_2 \times R_3$ space are given of the solution dynamics to the system for parameters in both regions I and II in figure 4.3. In region I, the solution converges to a stable steady state, while in region II the solution is a limit cycle about the equilibrium.

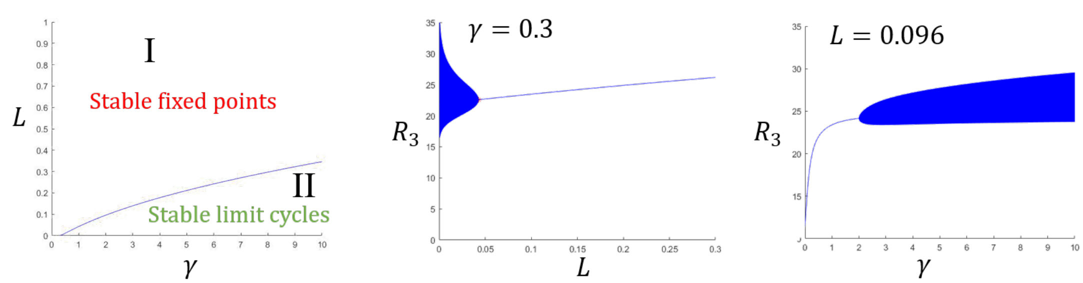

Figure 4.1: Bifurcation plots for $F(R_3) = 1 - \frac{R_3}{s}$ and $G(R_1) = L$. The middle figure demonstrates behavior in R_3 when traversing from region II to region I in the left figure with γ held constant, while the right figure demonstrates behavior in R_3 when traversing from region I to region II in the left figure with L held constant.

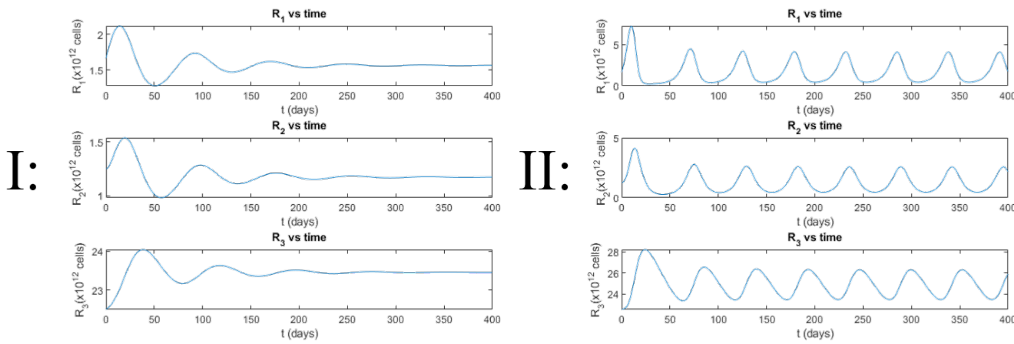

Figure 4.2: Plots of R_i vs. time for $F(R_3) = 1 - \frac{R_3}{s}$ and $G(R_1) = L$ for each of the regions in the bifurcation plane given in Figure 4.1.

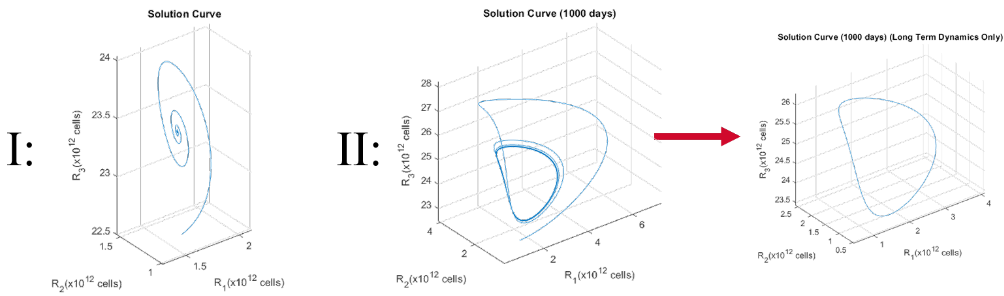

Figure 4.3: Solution curves for $F(R_3) = 1 - \frac{R_3}{s}$ and $G(R_1) = L$ in 3D space.

4.2 Analysis for Case 2: Hill-type F, Constant G

Here we have $F(R_3) = \frac{\theta^n}{\theta^n + {R_3}^n}$ and $G(R_1) = L$. In figure 4.4, we display bifurcation plots for the system, using parameter handles of γ and L, for parameter values in and around those given in table 2.5. We see the bifurcation lotus in the γ, L plane divides the space into two regions, the first of which (labeled I) corresponds to stable fixed points and the second of which (II) corresponds to stable limit cycles. This relationship is illustrated in figure 4.5. Finally, plots in $R_1 \times R_2 \times R_3$ space are given of the solution dynamics to the system for parameters in both regions I and II in figure 4.6. In region I, the solution converges to a stable steady state, while in region II the solution is a limit cycle about the equilibrium.

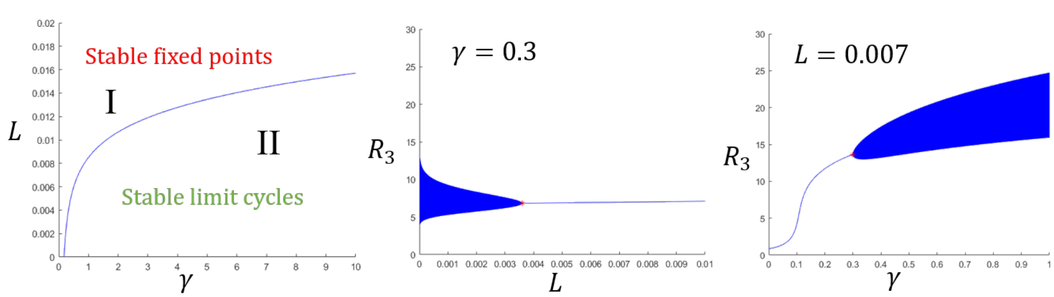

Figure 4.4: Bifurcation plots for $F(R_3) = \frac{\theta^n}{\theta^n + {R_3}^n}$ and $G(R_1) = L$. The right figure demonstrates behavior in R_3 when traversing from region II to region I in the left figure with γ held constant, while the right figure demonstrates behavior in R_3 when traversing from region I to region II in the left figure with L held constant.

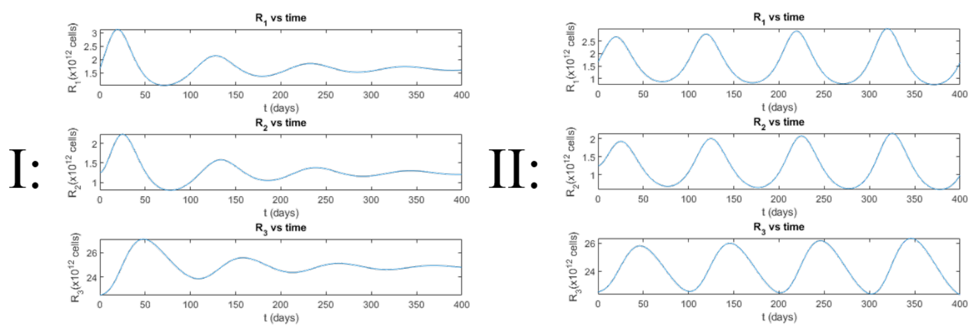

Figure 4.5: Plots of R_i vs. time for $F(R_3) = \frac{\theta^n}{\theta^n + {R_3}^n}$ and $G(R_1) = L$ for each of the regions in the bifurcation plane.

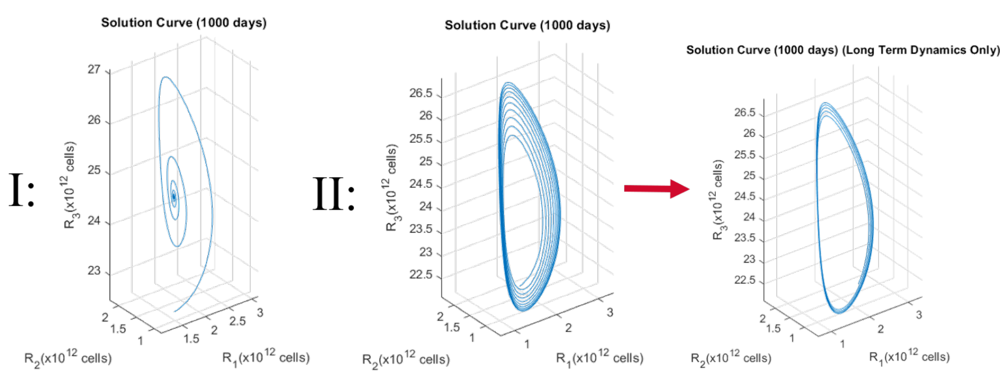

Figure 4.6: Solution curves for$F(R_3) = \frac{\theta^n}{\theta^n + {R_3}^n}$ and $G(R_1) = L$ in 3D space.

4.3 Analysis for Case 3: Linear F, Logistic G

Here we have $F(R_3) = 1 - \frac{R_3}{s}$ and $G(R_1) = \alpha R_1(1 - \frac{R_1}{K})$. In figure 4.7, we display bifurcation plots for the system, using parameter handles of γ and α, for parameter values in and around those given in table 2.5. We see the bifurcation lotus in the γ, α plane divides the space into two regions, the first of which (labeled I) corresponds to stable fixed points and the second of which (II) corresponds to stable limit cycles. This relationship is illustrated in figure 4.8. Finally, plots in $R_1 \times R_2 \times R_3$ space are given of the solution dynamics to the system for parameters in both regions I and II in figure 4.9. In region I, the solution converges to a stable steady state, while in region II the solution is a limit cycle about the equilibrium.

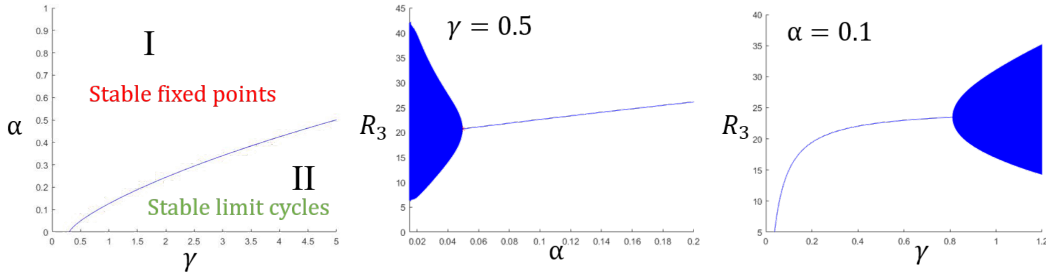

Figure 4.7: Bifurcation plots for $F(R_3) = 1 - \frac{R_3}{s}$ and $G(R_1) = \alpha R_1(1 - \frac{R_1}{K})$. The right figure demonstrates behavior in R_3 when traversing from region II to region I in the left figure with γ held constant, while the right figure demonstrates behavior in R_3 when traversing from region I to region II in the left figure with α held constant.

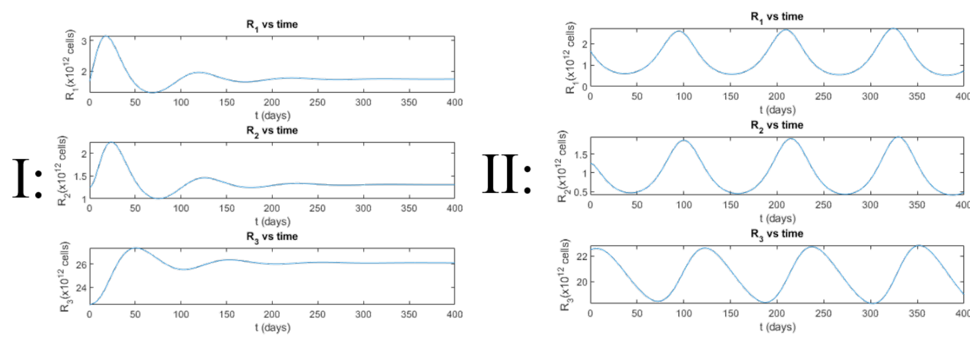

Figure 4.8: Plots of R_i vs. time for $F(R_3) = 1 - \frac{R_3}{s}$ and $G(R_1) = \alpha R_1(1 - \frac{R_1}{K})$ for each of the regions in the bifurcation plane.

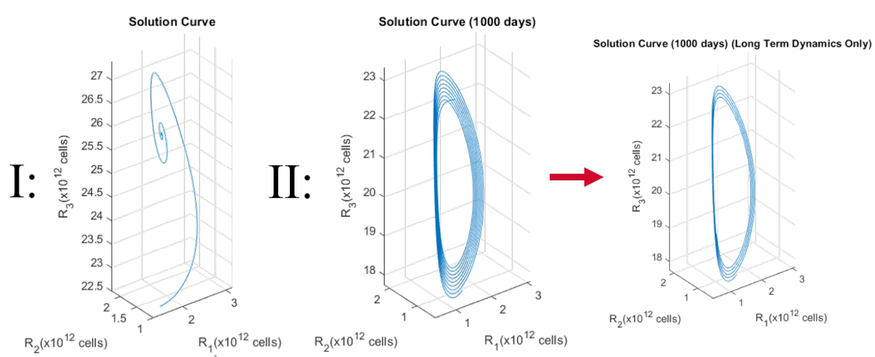

Figure 4.9: Solution curves for $F(R_3) = 1 - \frac{R_3}{s}$ and $G(R_1) = \alpha R_1(1 - \frac{R_1}{K})$ in 3D space.

4.4 Analysis for Case 4: Hill-type F, Logistic G

Here we have $F(R_3) = \frac{\theta^n}{\theta^n + {R_3}^n}$ and $G(R_1) = \alpha R_1(1 - \frac{R_1}{K})$. In figure 4.10, we display bifurcation plots for the system, using parameter handles of γ and α, for parameter values in and around those given in table 2.5. We see the bifurcation lotus in the γ,

α plane divides the space into two regions, the first of which (labeled I) corresponds to stable fixed points and the second of which (II) corresponds to stable limit cycles. This relationship is illustrated in figure 4.11. Finally, plots in $R_1 \times R_2 \times R_3$ space are given of the solution dynamics to the system for parameters in both regions I and II in figure 4.12. In region I, the solution converges to a stable steady state, while in region II the solution is a limit cycle about the equilibrium.

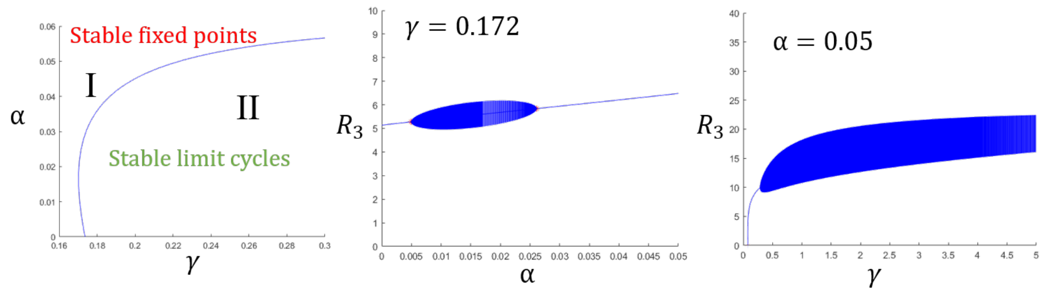

Figure 4.10: Bifurcation plots for $F(R_3) = \frac{\theta^n}{\theta^n + {R_3}^n}$ and $G(R_1) = \alpha R_1(1 - \frac{R_1}{K})$. The right figure demonstrates behavior in R_3 when traversing from region I through region II back to region I in the left figure with γ held constant, while the right figure demonstrates behavior in R_3 when traversing from region I to region II in the left figure with α held constant.

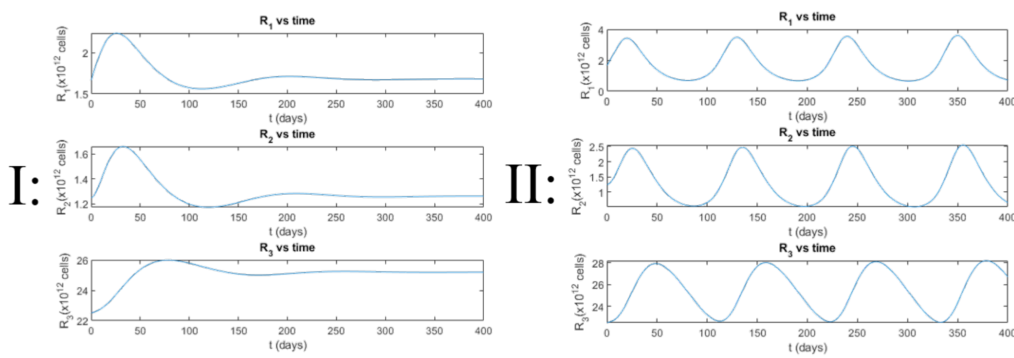

Figure 4.11: Plots of R_i vs. time for $F(R_3) = \frac{\theta^n}{\theta^n + {R_3}^n}$ and $G(R_1) = \alpha R_1(1 - \frac{R_1}{K})$ for each of the regions in the bifurcation plane.

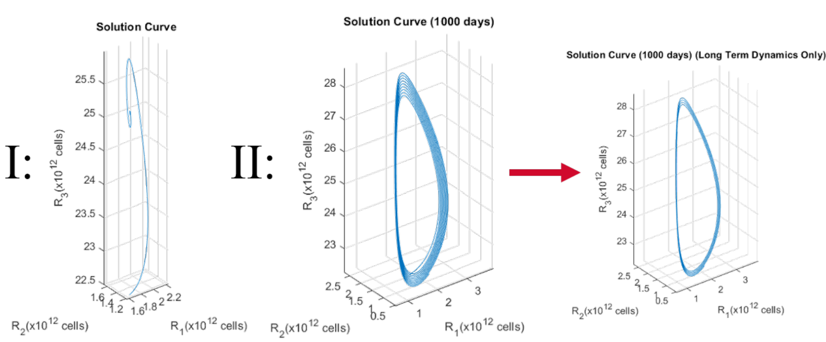

Figure 4.12: Solution curves for $F(R_3) = \frac{\theta^n}{\theta^n + {R_3}^n}$ and $G(R_1) = \alpha R_1(1 - \frac{R_1}{K})$ in 3D space.

Chapter 5

Applications to Blood Loss Systems, $H \neq 0$

Below we present several choices of H and the biological context which they may be used to model.

5.1 Constant Loss Function

A constant choice of H could be utilized in cases of constant bleeding or other loss due to disease. In figure 5.2, we display a numerical output for

$$H(R_3) = A$$

where $A = 0.25$ and all other parameters retain the values in table 2.5. In the figure, we observe R_i vs. time when the system is started from a perturbation at $t = 0$. We notice that the system settles to a steady state value smaller in magnitude than the case when $H = 0$.

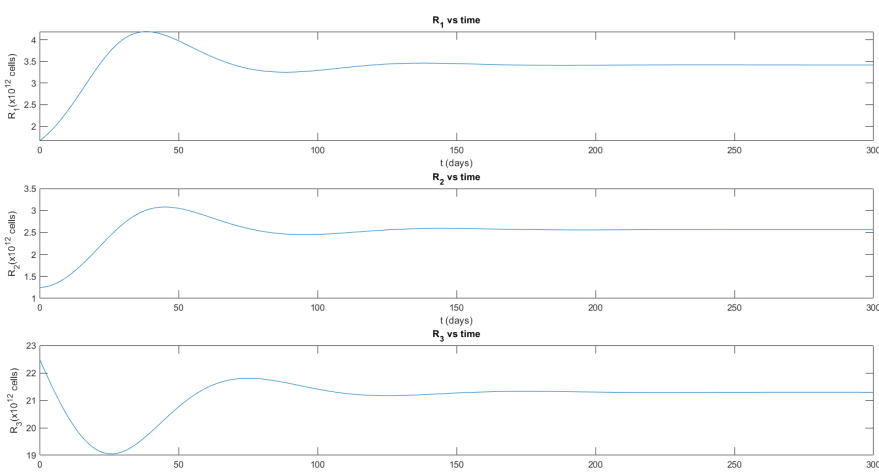

Figure 5.1: Plots of R_i vs. time for H as a constant function using human parameters.

5.2 Sinusoidal Loss Function

A sinusoidal choice of H could be used to model menstruation. In figure **??**, we display a numerical output for

$$H(R_3) = A|\sin(\pi t/30)|$$

where we use $A = 0.25$ and all other parameters retain the values in table 2.5. This periodic choice of H reaches its peak value of A every 30 days, modeling a monthly cycle. In the figure, we observe that R_3 settles down to fixed oscillations with period 30 days, matching the behavior of this choice of H.

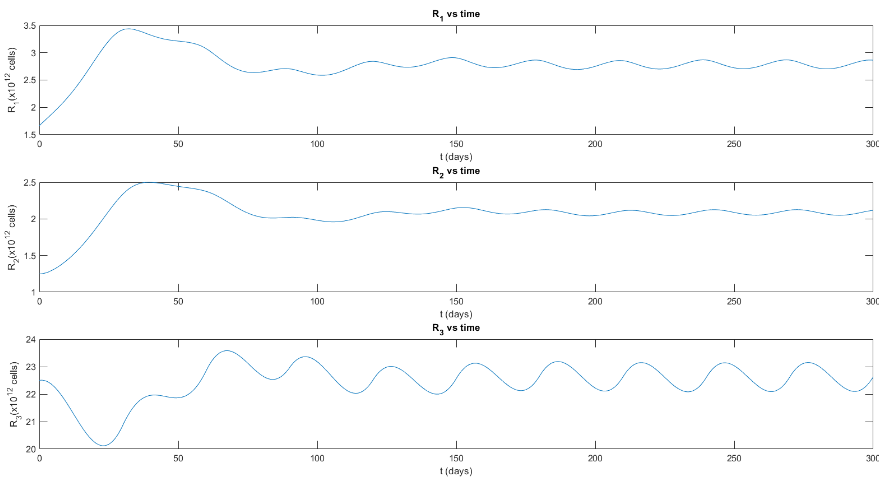

Figure 5.2: Plots of R_i vs. time for H as a sinusoidal function using human parameters. R_3 dynamics follow a period of 30 days, which is the same as the period of this choice of H.

5.3 Piecewise Loss Function

A piecewise choice of H could be used to model periodic loss, such as bloodletting or menstruation. In figure 5.3, we display a numerical output for

$$H(R_3) = \begin{cases} 0 & \text{if } (t \mod 30) < 24 \\ A & \text{else} \end{cases}$$

where we use $A = 0.25$ and all other parameters retain the values in table 2.5. This piecewise function gives a square wave following a monthly cycle. In the figure, we notice that R_3 exhibits jagged oscillations with period 30 days, following the periodic impulse behavior of this choice of H.

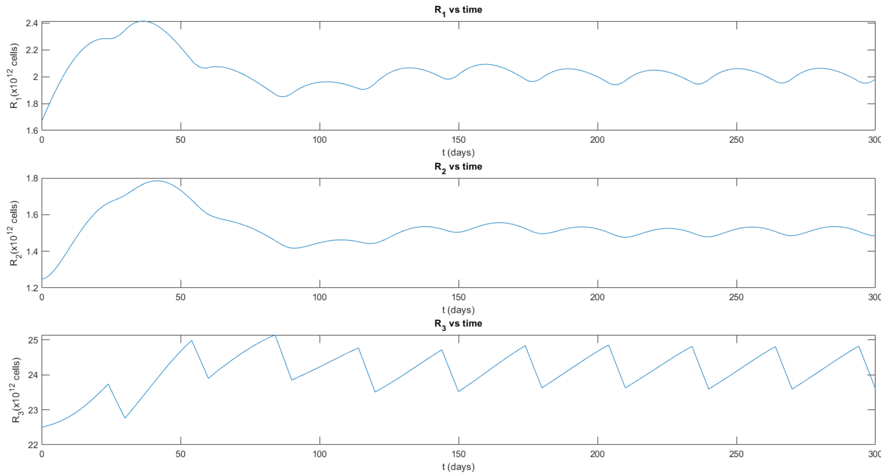

Figure 5.3: Plots of R_i vs. time for H as a piecewise function using human parameters. R_3 dynamics follow a period of 30 days, which is the same as the period of this choice of H.

While we have illustrated the dynamics for three examples of $H \neq 0$, we can extend this framework to a host of other possibilities. For example, adding a fourth variable for malaria could extend the applicability of the H function, allowing for modeling of malarial parasitemia.

Chapter 6

Discussion

In Chapter 4, we observed bifurcations for each of the four cases of functional choices examined within this thesis. However, in the first case, we notice that the parameter windows necessary for these bifurcations fall outside those given in Table 2.5. The other cases, however, exhibit bifurcations within these biologically reasonable windows, showing that this model of blood dynamics can exhibit oscillatory dynamics for perturbed parameter values. We saw that all four cases exhibited a linearly stable region (within the desired parameter region) with a unique, nontrivial steady state. For the case where G is modeled by a logistic function, this steady state only existed when certain threshold conditions that coincided with the instability of the trivial steady state were met. In Chapter 5, we saw how the system 2.1 can exhibit oscillatory dynamics for an appropriate choice of ongoing loss in the functional H.

Results for mice hold by rescaling of the values obtained for humans. However, the production of precursor cells in the spleen by mice provides an interesting dynamic to the feedback function, as splenic regeneration helps boost feedback following a blood loss. It remains to be seen whether the feedback functions discussed in this thesis can account for this boosted regeneration, or if a second feedback function representing this phenomena would be the more appropriate choice.

In this thesis, we set out to create a generalized model of erythropoiesis during blood loss. Above, we discussed several potential applications of this model to Polycythemia Vera, menstruation, and bloodletting. We examined the impact of parameters on system dynamics and explored the impact of choosing different functions to capture the processes of feedback and production. We mathematically observed the similarity in dynamics among four different functional choices, seeing that a variety of functions can be used to caption the dynamics of erythropoiesis. We also saw how the loss function H can be extended to specific loss scenarios. In the future, linking this function to malarial parasitemia by making H a function of both R_3 and parasitemia could prove useful in modeling the impact of this disease on the blood.

Chapter 7

Appendix

7.1 Mathematics in Original Variables

Proposition 4. *We state the characteristic polynomial $p_J(\lambda)$ of (2.1) in (7.1):*

$$\begin{aligned} p_J(\lambda) &= -\beta^2 k_1 k_2 \gamma F'(R_3) R_1 - (\beta k_2 + \lambda)(\beta a + H'(R_3) + \lambda)(\beta G'(R_1) - \beta k_1 + \gamma F(R_3) - \lambda) \\ &= \lambda^3 - \lambda^2[\beta G'(R_1) - \beta k_1 + \gamma F(R_3) - \beta k_2 - \beta a - H'(R_3)] \\ &- \lambda[(\beta G'(R_1) - \beta k_1 + \gamma F(R_3))(\beta k_2 + \beta a + H'(R_3)) - \beta k_2(\beta a + H'(R_3))] \\ &- [\beta^2 k_1 k_2 \gamma F'(R_3) R_1 + \beta k_2(\beta a + H'(R_3))(\beta G'(R_1) - \beta k_1 + \gamma F(R_3))] \end{aligned} \tag{7.1}$$

The characteristic polynomial in (7.1) can be written in the form $\lambda^3 + P\lambda^2 + Q\lambda + R = 0$, where:

$$\begin{aligned} P &= -\beta G'(R_1) + \beta k_1 + \beta\mu_1 - \gamma F(R_3) + \beta k_2 + \beta\mu_2 + \beta\mu_3 + H'(R_3) \\ Q &= (-\beta G'(R_1) + \beta k_1 + \beta\mu_1 - \gamma F(R_3))(\beta k_2 + \beta\mu_2 + \beta\mu_3 + H'(R_3)) + (\beta k_2 + \beta\mu_2)(\beta\mu_3 + H'(R_3)) \\ R &= -\beta^2 k_1 k_2 \gamma F'(R_3) R_1 - (\beta k_2 + \beta\mu_2)(\beta\mu_3 + H'(R_3))(\beta G'(R_1) - \beta k_1 - \beta\mu_1 + \gamma F(R_3)) \end{aligned}$$

Notice that if $(\beta G'(R_1) - \beta k_1 - \beta\mu_1 + \gamma F(R_3)) \leq 0$; $P > 0$, $Q > 0$, and $R > 0$ are guaranteed. By Proposition 2 and Proposition 1, this condition will be met for some values of $\vec{R} = (R_1, R_2, R_3)$ independent of parameters.

Theorem 12. *If the characteristic polynomial, written $\lambda^3 + P\lambda^2 + Q\lambda + R = 0$, of a system of ordinary differential equations has the property that $R = PQ$ for some value $\vec{R}_h$ in the system, then the system exhibits a Hopf Bifurcation at $\vec{R}_h$.*

Proof. See Ngonghala et al. [12]. □

We will demonstrate that $\vec{R}_h$ exists for (2.1) and define the following groupings:

$$\begin{aligned} X &= (-\beta G'(R_1) + \beta k_1 - \gamma F(R_3)) \quad & Y &= (\beta k_2 + \beta\mu + H'(R_3)) \\ Z &= -\beta^2 k_1 k_2 \gamma F'(R_3) R_1 & W &= \beta k_2(\beta\mu + H'(R_3)) = \beta k_2(Y - \beta k_2) \end{aligned} \tag{7.2}$$

From (7.2) and Proposition 4, we have:

$$P = X + Y \quad Q = XY + W \quad R = Z + WX \quad PQ = X^2Y + Y^2X + WX + WY \tag{7.3}$$

Theorem 13. *The system (2.1) can exhibit a Hopf Bifurcation for biologically reasonable parameter and function choices.*

Proof. By (7.3) and Theorem 12, $\vec{R}_h$ will exist when $Z = X^2Y + Y^2X + WY = Y(X^2 + XY + W)$. Using the nondimensionalization given in Section 3.2, this condition can be simplified to the following, with x and y defined:

$$-\mu k_1 k_2 f'(r_3) r_1 = (k_2 + k_1 x)(k_2 + y)(k_1 x + y) \tag{7.4}$$

$$x = (-f(r_3) - g'(r_1) + 1) \qquad\qquad y = (\mu + h'(r_3))$$

Therefore the following equality will hold at the Hopf Bifurcation point, $\vec{R}_h$:

$$\frac{PQ}{R} = \frac{(k_2 + k_1 x)(k_2 + y)(k_1 x + y)}{-\mu k_1 k_2 f'(r_3) r_1} \tag{7.5}$$

If (2.1) has a biologically reasonable interpretation for both $\frac{PQ}{R} >> 1$ and $\frac{PQ}{R} << 1$, then by the intermediate value theorem, $\frac{PQ}{R} = 1$, and thus the Hopf Bifurcation point $\vec{R}_h$, can exist.

When $R_1 \to \infty$, if $x > 0$, then $\frac{PQ}{R} >> 1$. If $x < 0$ and $k_2 + k_1 x < 0$, meanwhile, as h is bounded and increasing (Proposition 3) we may find an r_3 such that $\mu + h'(r_3) \leq k_2$ since $\mu < k_2$ by design. This means the numerator will still be positive, and $\frac{PQ}{R} >> 1$. This state corresponds to low R_1 levels - corresponding to large blood loss or death.

In the alternate case of $\frac{PQ}{R} << 1$, we take $R_1 > R_1^*$, where R_1^* is the steady state value. Then assume $G'(R_1) \leq 0$, $G'(R_1) \to 0$ as $R_1 \to \infty$, and $f(r_3) \geq 1$. These conditions result in $\frac{PQ}{R} << 1$ for large R_1, so we see this state corresponds to high R_1 values and an overabundance of precursor cells, in contrast to the previous situations.

Thus we see that these two biological events - low precursor blood cell count or high precursor blood cell count - swing (2.1) away from the situation of $\frac{PQ}{R} = 1$ and the Hopf lotus. □

7.2 MATLAB Code

MATLAB code used to generate the graphics and numerical results in the preceding chapters is given, excluding MATCONT results, to which credit goes to [11].

7.2.1 Code for Chapter 3.3

To generate the existence plots given in Chapters 3.3.2 and 3.3.4 above, we use the inputs `(1, 1/8, 1/6, 1/120, 0.3, 24.98, 12.5, 5, .21, .166, 6.66, 0, 0)` on the functions presented in the MATLAB code below.

```
function IntersectPlotter2(beta, k1, k2, mu3, gamma, s, theta, ...
    n, L, alpha, K, mu1, mu2)
l=1;
a3=[350 604.8 700];
rho=[12 36 100];
for j=1:3
     for k=1:3

          Δ1 = (k1+mu1)/mu3;
          Δ2 = (k2+mu2)/mu3;

          R3=18:13/99:31;
          r3=R3/theta;
          r1=r3*Δ2/a3(j);
          n=1:5;

          lo=(rho(k)-Δ1).*r1+1;

          subplot(3,3,l)

          plot(r1,lo)

          hold on
          for i=1:5

               ho=-Δ1*(a3(j)/Δ2)^n(i).* ...
                   r1.^(n(i)+1)+(a3(j)/Δ2)^n(i).*r1.^n(i);

               plot(r1,-ho)

          end
          xlabel('r_1'); %ylabel();
          title(sprintf("%s = %s, %s = ...
               %s",'a',num2str(a3(j)),'\rho',num2str(rho(k))));
          hold off
          ylim([min(lo)-2 max(lo)+2])
          lgd=legend('V(r_1)','U(r_1), n=1','U(r_1), n=2','U(r_1), ...
               n=3','U(r_1), n=4','U(r_1), n=5','Location','best');
          lgd.NumColumns = 3;
          l=l+1;
     end
end
sgtitle("Intersection(s) of U(r_1)=\Δ_1(a/\Δ_2)^n ...
    r_1^{n+1}-(a/\Δ_2)^n r_1^n and V(r_1)=1+(\rho-\Δ_1)r_1 for ...
    varying n")
end

```

```
%%%%%%%%

function IntersectPlotter4a(beta, k1, k2, mu3, gamma, s, theta, ...
    n, L, alpha, K, mu1, mu2)
l=1;
a4=[90 159.84 180];
rho=[12 36 80];
%w=[6 19.92 40]
for j=1:3
    for k=1:3

        ∆1 = (k1+mu1)/mu3;
        ∆2 = (k2+mu2)/mu3;

        w=alpha/mu3;

        R3=18:13/99:31;
        r3=R3/theta;
        r1=r3*∆2/a4(j);
        n=1:5;

        lo=(rho(k)+w-∆1)-w.*r1;

        subplot(3,3,l)

        plot(r1,lo)

        hold on
        for i=1:5

            ho=-w*(a4(j)/∆2)^n(i).*r1.^(n(i)+1) ...
                +(w-∆1)*(a4(j)/∆2)^n(i).*r1.^n(i);

            plot(r1,-ho)

        end
        xlabel('r_1'); %ylabel();
        title(sprintf("%s = %s, %s = %s, %s = ...
            %s",'a',num2str(a4(j)),'\rho',num2str(rho(k)),'\omega', ...
            num2str(w)));
        hold off
        ylim([min(lo)-2 max(lo)+2])
        lgd=legend('V(r_1)','U(r_1), n=1','U(r_1), n=2','U(r_1), ...
            n=3','U(r_1), n=4','U(r_1), n=5','Location','best');
        lgd.NumColumns = 3;
        l=l+1;
    end
end
sgtitle("Intersection(s) of U(r_1)=\omega (a/\∆_2)^n ...
    r_1^{n+1}-(\omega - \∆_1)(a/\∆_2)^n r_1^n and V(r_1)=(\rho+ ...
    \omega - \∆_1)- \omega r_1 for varying n")
end

function IntersectPlotter4b(beta, k1, k2, mu3, gamma, s, theta, ...
```

```
    n, L, alpha, K, mu1, mu2)
l=1;
%a4=[90 159.84 180];
rho=[12 36 80];
w=[6 19.92 21];
for j=1:3
    for k=1:3

        Δ1 = (k1+mu1)/mu3;
        Δ2 = (k2+mu2)/mu3;

        a4=(k1*k2*K)/(mu3.^2*theta);

        R3=18:13/99:31;
        r3=R3/theta;
        r1=r3*Δ2/a4;
        n=1:5;

        lo=(rho(k)+w(j)-Δ1)-w(j).*r1;

        subplot(3,3,l)

        plot(r1,lo)

        hold on
        for i=1:5

            ho=-w(j)*(a4/Δ2)^n(i).*r1.^(n(i)+1) ...
                +(w(j)-Δ1)*(a4/Δ2)^n(i).*r1.^n(i);

            plot(r1,-ho)

        end
        xlabel('r_1'); %ylabel();
        title(sprintf("%s = %s, %s = %s, %s = ...
            %s",'a',num2str(a4),'\rho',num2str(rho(k)),'\omega', ...
            num2str(w(j))));
        hold off
        ylim([min(lo)-2 max(lo)+2])
        lgd=legend('V(r_1)','U(r_1), n=1','U(r_1), n=2','U(r_1), ...
            n=3','U(r_1), n=4','U(r_1), n=5','Location','best');
        lgd.NumColumns = 3;
        l=l+1;
    end
end
sgtitle("Intersection(s) of U(r_1)=\omega (a/\Δ_2)^n ...
    r_1^{n+1}-(\omega - \Δ_1)(a/\Δ_2)^n r_1^n and V(r_1)=(\rho+ ...
    \omega - \Δ_1)- \omega r_1 for varying n")
end

function IntersectPlotter(beta, k1, k2, mu3, gamma, s, theta, n, ...
    L, alpha, K, mu1, mu2)
l=1;
a4=[90 159.84 180];
```

```
%rho=[12 36 80];
w=[6 19.92 21];
for j=1:3
    for k=1:3

        Δ1 = (k1+mu1)/mu3;
        Δ2 = (k2+mu2)/mu3;
        rho=gamma/(beta*mu3);

        R3=18:13/99:31;
        r3=R3/theta;
        r1=r3*Δ2/a4(k);
        n=1:5;

        lo=(rho+w(j)-Δ1)-w(j).*r1;

        subplot(3,3,l)

        plot(r1,lo)

        hold on
        for i=1:5

            ho=-w(j)*(a4(k)/Δ2)^n(i).*r1.^(n(i)+1) ...
                +(w(j)-Δ1)*(a4(k)/Δ2)^n(i).*r1.^n(i);

            plot(r1,-ho)

        end
        xlabel('r_1'); %ylabel();
        title(sprintf("%s = %s, %s = %s, %s = ...
            %s",'a',num2str(a4(k)),'\rho',num2str(rho),'\omega', ...
            num2str(w(j))));
        hold off
        ylim([min(lo)-2 max(lo)+2])
        lgd=legend('V(r_1)','U(r_1), n=1','U(r_1), n=2','U(r_1), ...
            n=3','U(r_1), n=4','U(r_1), n=5','Location','best');
        lgd.NumColumns = 3;
        l=l+1;
    end
end
sgtitle("Intersection(s) of U(r_1)=\omega (a/\Δ_2)^n ...
    r_1^{n+1}-(\omega - \Δ_1)(a/\Δ_2)^n r_1^n and V(r_1)=(\rho+ ...
    \omega - \Δ_1)- \omega r_1 for varying n")
end
```

7.2.2 Code for Chapter 3.4

To output the figures displayed in Chapter 3.4, we call the function `CharPolySurfPlotter`, which uses the functions `CharPolySurf` and `CharPolyCoeffs` in its operation. Varying the parameters `choice` and `coeff` and with the other inputs given by `Tests=CharPolySurfPlotter,1,coeff,1,20,[0 .1875 3/8],[0 225/1200 450/1200],[2,5,10],[.01 .05 .1]);`, we obtained the plots.

```
function ...
    Tests=CharPolySurfPlotter(choice,sub,coeff,tester,size,mu1,mu2,n,z)

%choice: which functional choices for f and g to use
%sub: parameter for plots
%coeff: which plot to print
%tester: boolean for returning checks on P, Q, and R
%size: number of points to plot
%mu1, mu2, n, z: test values for various parameters

if choice=="1"
     lb(1)="a";
     lb(2)="\rho";
elseif choice == "3"
     lb(1)="\omega";
     lb(2)="\rho";
elseif choice=="2"
     lb(1)="a";
     lb(2)="\rho";
elseif choice=="4"
     lb(1)="a";
     lb(2)="\rho";
end
k=1;
figure
for i=1:3
     for j=1:3
         if sub==1
             [x,y,P,Q,R,Δ1,Δ2,n1,w]=CharPolySurf(1, 1/8, 1/6, ...
                 1/120, .3, 24.98, 12.5, 5, 0.21, .166, 6.66, ...
                 mu1(i), mu2(j), .25, choice, [1.6653 1.249 ...
                 22.5], 0, 3000,0,0, size);
             xa="\Δ_1";
             xv=Δ1;
             ya="\Δ_2";
             yv=Δ2;
         elseif sub==2
             [x,y,P,Q,R,Δ1,Δ2,n1,w]=CharPolySurf(1, 1/8, 1/6, ...
                 1/120, .3, 24.98, 8.9, n(j), 0.1, .22, 6.66, ...
                 mu1(i), 0, .25, choice, [1.6653 1.249 22.5], 0, ...
                 3000,0,0, size);
             xa="\Δ_1";
             xv=Δ1;
             ya="n";
             yv=n1;
         elseif sub==3
             [x,y,P,Q,R,Δ1,Δ2,n1,w]=CharPolySurf(1, 1/8, 1/6, ...
                 1/120, .3, 24.98, 8.9, n(j), 0.1, .22, 6.66, 0, ...
                 mu2(i), .25, choice, [1.6653 1.249 22.5], 0, ...
                 3000,0,0, size);
             xa="\Δ_2";
```

```
            xv=∆2;
            ya="n";
            yv=n1;
        elseif sub==4
            [x,y,P,Q,R,∆1,∆2,n1,w]=CharPolySurf(1, 1/8, 1/6, ...
               1/120, .3, 24.98, 8.9, n(j), 0.1, z(i), 6.66, 0, ...
               0, .25, choice, [1.6653 1.249 22.5], 0, ...
               3000,0,0, size);
            xa="\omega";
            xv=w;
            ya="n";
            yv=n1;
        end
        subplot(3,3,k)
        if coeff=='P'
            surf(x,y,P)

            if choice=="3"
                xPlane = [x(1,1) ...
                   x(length(x(1,:)),length(x(1,:))) ...
                   x(length(x(1,:)),length(x(1,:))) x(1,1)];
                yPlane1 = ∆1-xPlane;
                zPlane = [-10000 -10000 10000 10000];
                hold on;
                patch(xPlane, yPlane1, zPlane, 'r', 'FaceAlpha', ...
                   0.5);
                hold off
                xlim([x(1,1) x(length(x(1,:)),length(x(1,:)))])
                ylim([y(1,1) y(length(y(:,1)),length(y(:,1)))])
                zlim([min(min(P, [], 'all'),-10) max(P, [], 'all')])
            end
            hold on;
            patch([x(length(x(1,:)),length(x(1,:))) x(1,1) ...
               x(1,1) x(length(x(1,:)),length(x(1,:)))], ...
               [y(length(y(:,1)),length(y(:,1))) ...
               y(length(y(:,1)),length(y(:,1))) y(1,1) y(1,1)], ...
               [0 0 0 0], 'g', 'FaceAlpha', 0.5);
            hold off

            xlabel(lb(1)); ylabel(lb(2)); zlabel(coeff);
            title(sprintf('%s = %s, %s = ...
               %s',xa,num2str(xv),ya,num2str(yv)));
        elseif coeff=='Q'
            surf(x,y,Q)

            if choice=="3"
                xPlane = [x(1,1) ...
                   x(length(x(1,:)),length(x(1,:))) ...
                   x(length(x(1,:)),length(x(1,:))) x(1,1)];
                yPlane1 = ∆1-xPlane;
                zPlane = [-10000 -10000 10000 10000];
                hold on;
                patch(xPlane, yPlane1, zPlane, 'r', 'FaceAlpha', ...
                   0.5);
```

```
                hold off
                xlim([x(1,1) x(length(x(1,:)),length(x(1,:)))])
                ylim([y(1,1) y(length(y(:,1)),length(y(:,1)))])
                zlim([min(Q, [], 'all') max(Q, [], 'all')])
            end
            hold on;
            patch([x(length(x(1,:)),length(x(1,:))) x(1,1) ...
                x(1,1) x(length(x(1,:)),length(x(1,:)))], ...
                [y(length(y(:,1)),length(y(:,1))) ...
                y(length(y(:,1)),length(y(:,1))) y(1,1) y(1,1)], ...
                [0 0 0 0], 'g', 'FaceAlpha', 0.5);
            hold off

            xlabel(lb(1)); ylabel(lb(2)); zlabel(coeff);
            title(sprintf('%s = %s, %s = ...
                %s',xa,num2str(xv),ya,num2str(yv)));
        elseif coeff=='R'
            surf(x,y,R)

            if choice=="3"
                xPlane = [x(1,1) ...
                    x(length(x(1,:)),length(x(1,:))) ...
                    x(length(x(1,:)),length(x(1,:))) x(1,1)];
                yPlane1 = ∆1-xPlane;
                zPlane = [-10000 -10000 10000 10000];
                hold on;
                patch(xPlane, yPlane1, zPlane, 'r', 'FaceAlpha', ...
                    0.5);
                hold off
                xlim([x(1,1) x(length(x(1,:)),length(x(1,:)))])
                ylim([y(1,1) y(length(y(:,1)),length(y(:,1)))])
                zlim([min(R, [], 'all') max(R, [], 'all')])
            end
            hold on;
            patch([x(length(x(1,:)),length(x(1,:))) x(1,1) ...
                x(1,1) x(length(x(1,:)),length(x(1,:)))], ...
                [y(length(y(:,1)),length(y(:,1))) ...
                y(length(y(:,1)),length(y(:,1))) y(1,1) y(1,1)], ...
                [0 0 0 0], 'g', 'FaceAlpha', 0.5);
            hold off

            xlabel(lb(1)); ylabel(lb(2)); zlabel(coeff);
            title(sprintf('%s = %s, %s = ...
                %s',xa,num2str(xv),ya,num2str(yv)));

        elseif coeff=="PQ/R"

            surf(x,y,P.*Q./R);

            if choice=="3"
                xPlane = [x(1,1) ...
                    x(length(x(1,:)),length(x(1,:))) ...
                    x(length(x(1,:)),length(x(1,:))) x(1,1)];
                yPlane1 = ∆1-xPlane;
```

```
                    zPlane = [-10000 -10000 10000 10000];
                    hold on;
                    patch(xPlane, yPlane1, zPlane, 'r', 'FaceAlpha', ...
                        0.5);
                    hold off
                    xlim([x(1,1) x(length(x(1,:)),length(x(1,:)))])
                    ylim([y(1,1) y(length(y(:,1)),length(y(:,1)))])
                    zlim([min(R, [], 'all') max(R, [], 'all')])
                end

                zlim([0 1])

                xlabel(lb(1)); ylabel(lb(2)); zlabel("PQ/R");
                title(sprintf('%s = %s, %s = ...
                    %s',xa,num2str(xv),ya,num2str(yv)));

            end

            if tester==1
                Tests(k,:)=CharPolyCoeffs(x,y,P,Q,R,Δ1,choice,size);
            else
                Tests=0;
            end
            k=k+1;
        end
end
sgtitle("Plots of "+coeff+" for varying "+lb(1)+", "+lb(2)+", ...
    "+xa+", and "+ya+" for case "+choice)
end
```

```
function [x,y,P,Q,R,Δ1,Δ2,n,w]=CharPolySurf(beta, k1, k2, mu3, ...
    gamma, s, theta, n, L, alpha, K, mu1, mu2, A, choice, initV, ...
    ts, tf, T, eps, size)

%input (beta, k1, k2, mu3, gamma, s, theta, n, L, alpha, K, mu1, ...
    mu2, A, choice, initV, ts, tf, T, eps, size)

% beta - Individual blood regeneration amplifying factor ...
    independent of fractional blood loss
% k1 - Transition rate between R1 and R2 (1/8 in humans)
% k2 - Transition rate between R2 and R3 (1/6 in humans)
% mu3 - Death rate of R3 (1/120 in humans)
% gamma - Individual blood regeneration amplifying factor ...
    dependent on fractional blood loss
% s - Mean steady state value of R3
% theta - Saturation constant for R3 feedback
% n - Sensitivity of feedback with respect to changes in ...
    population size
% L - Constant growth rate of R1
% alpha - Logistic growth rate
% K - Maximum stimulated size of R1 population
% mu1 - Natural apoptosis rate of R1
```

```
% mu2 - Natural apoptosis rate of R2
% A - Constant loss from R3
% choice - 1, 2, 3, or 4 for different F and G functions
% initV - Initial value starting conditions
% ts - Time at which to begin simulation
% tf - Time at which to end simulation
% T - Unused time variable
% eps - Unused tolerance
% size - Number of points to plot

%%nondimensional parameters

Δ1 = (k1+mu1)/mu3;
Δ2 = (k2+mu2)/mu3;
rho=gamma/(beta*mu3);
a1=(k1*k2*L)/(mu3.^3*s);
a2=(k1*k2*K)/(mu3.^2*s);
a3=(k1*k2*L)/(mu3.^3*theta);
a4=(k1*k2*K)/(mu3.^2*theta);
w=alpha/mu3;
r11=(rho - Δ1 + sqrt((rho-Δ1).^2+4*rho*a1/Δ2))/(2*rho*a1/Δ2);
r31=r11*a1/Δ2;

%initializing arrays
P=zeros(size);
Q=zeros(size);
R=zeros(size);

%linear f constant g
if choice=="1"
    a1_m=160:390/(size-1):550;
    rho_m=1:239/(size-1):240;
    for j=1:size
        for i=1:size

            r11m=(rho_m(i) - Δ1 + ...
               sqrt((rho_m(i)-Δ1)^2+4*rho_m(i)*a1_m(j)/Δ2))/(2*rho_m(i)*a1_m(j)/Δ2);
            r31m=r11m*a1_m(j)/Δ2;

            combination=Δ1 - rho_m(i) + rho_m(i)*r31m;

            P(i,j) = 1+Δ2 + combination;
            Q(i,j) = Δ2 + (Δ2 + 1)*(combination);
            R(i,j) = a1_m(j)*rho_m(i)*r11m + Δ2*(combination);

        end
    end
    [x,y] = meshgrid(a1_m,rho_m);

%hill-type f, constant g
elseif choice=="2"

    a3_m=330:720/(size-1):1050;
    rho_m=1:239/(size-1):240;
```

```
    r13m=0;
    for j=1:size
        for i=1:size
            %computing equilibrium point numerically
            poly=zeros(1,n+2);
            poly(1)=-Δ1*(a3_m(j)/Δ2)^n;
            poly(2)=(a3_m(j)/Δ2)^n;
            poly(n+1)=rho_m(i)-Δ1;
            poly(n+2)=1;
            rooty=roots(poly);
            posrootcount=0;

            for rt=1:n+1
                if real(rooty(rt))>0 && imag(rooty(rt))==0
                    r13m=real(rooty(rt));
                    posrootcount=posrootcount+1;
                end
                if posrootcount>1
                    fprintf('Additional root of %13.2e found at ...
                        a= %13.2e and rho = ...
                        %13.2e\n',r13m,a3_m(j),rho_m(i));
                end
            end
            if posrootcount==0
                fprintf('No roots found at a= %13.2e and rho = ...
                    %13.2e with Δ1 = %13.2e and Δ2 = ...
                    %13.2e\n',a3_m(j),rho_m(i),Δ1,Δ2);
            end

            r33m=r13m*a3_m(j)/Δ2;

            combination=Δ1 - rho_m(i)/(1+r33m^n);

            P(i,j) = 1+Δ2 + combination;
            Q(i,j) = Δ2 + (Δ2 + 1)*(combination);
            R(i,j) = a3_m(j)*rho_m(i)*r13m + Δ2*(combination);

        end
    end
    [x,y] = meshgrid(a3_m,rho_m);

%linear f, logistic g
elseif choice=="3"
    w_m=5:45/(size-1):50;
    rho_m=1:239/(size-1):240;
    for j=1:size
        for i=1:size

            r11m=(rho_m(i) - Δ1 + w_m(j))/(w_m(j)+rho_m(i)*a2/Δ2);
            r31m=r11m*a2/Δ2;

            combination=2*w_m(j)*r11m - w_m(j) + Δ1 - rho_m(i) + ...
                rho_m(i)*r31m;

```

```
            P(i,j) = 1+∆2 + combination;
            Q(i,j) = ∆2 + (∆2 + 1)*(combination);
            R(i,j) = a2*rho_m(i)*r11m + ∆2*(combination);

        end
    end
    [x,y] = meshgrid(w_m,rho_m);

%hill-type f, logistic g
elseif choice=="4"

    a4_m=90:200/(size-1):290;
    rho_m=1:239/(size-1):240;
    r14m=0;
    for j=1:size
        for i=1:size
            %computing equilibrium point numerically
            poly=zeros(1,n+3);
            poly(1)=-w*(a4_m(j)/∆2)^n;
            poly(2)=(w-∆1)*(a4_m(j)/∆2)^n;
            poly(n+1)=-w;
            poly(n+2)=rho_m(i)+w-∆1;
            rooty=roots(poly);
            posrootcount=0;

            for rt=1:n+2
                if real(rooty(rt))>0 && imag(rooty(rt))==0
                    r14m=real(rooty(rt));
                    posrootcount=posrootcount+1;
                end
                if posrootcount>1
                    fprintf('Additional root of %13.2e found at ...
                        a= %13.2e and rho = ...
                        %13.2e\n',r14m,a4_m(j),rho_m(i));
                end
            end
            if posrootcount==0 && ∆1>(rho_m(i)+w) %parameter ...
                range where there is no existence of the ...
                equilibrium point by Descartes
                P(i,j) = NaN;
                Q(i,j) = NaN;
                R(i,j) = NaN;
            else

                r34m=r14m*a4_m(j)/∆2;

                combination=2*w*r14m - w + ∆1 - rho_m(i)/(1+r34m^n);

                P(i,j) = 1+∆2 + combination;
                Q(i,j) = ∆2 + (∆2 + 1)*(combination);
                R(i,j) = a4_m(j)*rho_m(i)*r14m + ∆2*(combination);
            end
        end
    end
```

```
    [x,y] = meshgrid(a4_m,rho_m);

end
end
```

```
function tests = CharPolyCoeffs(x,y,P,Q,R,Δ1,choice,size)
X=zeros(size);
if choice=="1"

for i1=1:size
    for j1=1:size
        if P(i1,j1)<0 && Q(i1,j1)>0 && R(i1,j1)<0
            X(i1,j1)=1;
        elseif P(i1,j1)<0 && Q(i1,j1)>0 && R(i1,j1)>0
            X(i1,j1)=2;
        elseif P(i1,j1)<0 && Q(i1,j1)<0 && R(i1,j1)<0
            X(i1,j1)=3;
        elseif P(i1,j1)<0 && Q(i1,j1)<0 && R(i1,j1)>0
            X(i1,j1)=4;
        elseif P(i1,j1)>0 && Q(i1,j1)>0 && R(i1,j1)<0
            X(i1,j1)=5;
        elseif P(i1,j1)≥0 && Q(i1,j1)≥0 && R(i1,j1)≥0
            X(i1,j1)=6;
        elseif P(i1,j1)>0 && Q(i1,j1)<0 && R(i1,j1)<0
            X(i1,j1)=7;
        elseif P(i1,j1)>0 && Q(i1,j1)<0 && R(i1,j1)>0
            X(i1,j1)=8;
        else
            X(i1,j1)=0;
        end
    end
end

for i2=0:8
    tests(i2+1)=ismember(i2,X);
end

elseif choice=="3"
for i1=1:size
    for j1=1:size
        if P(i1,j1)<0 && Q(i1,j1)>0 && R(i1,j1)<0 && ...
           x(i1,j1)+y(i1,j1)>Δ1
            X(i1,j1)=1;
        elseif P(i1,j1)<0 && Q(i1,j1)>0 && R(i1,j1)>0 && ...
           x(i1,j1)+y(i1,j1)>Δ1
            X(i1,j1)=2;
        elseif P(i1,j1)<0 && Q(i1,j1)<0 && R(i1,j1)<0 && ...
           x(i1,j1)+y(i1,j1)>Δ1
            X(i1,j1)=3;
        elseif P(i1,j1)<0 && Q(i1,j1)<0 && R(i1,j1)>0 && ...
           x(i1,j1)+y(i1,j1)>Δ1
            X(i1,j1)=4;
```

```
        elseif P(i1,j1)>0 && Q(i1,j1)>0 && R(i1,j1)<0 && ...
            x(i1,j1)+y(i1,j1)>∆1 %&& z(i1,j1) ==1
            X(i1,j1)=5;
        elseif P(i1,j1)>0 && Q(i1,j1)>0 && R(i1,j1)>0 && ...
            x(i1,j1)+y(i1,j1)>∆1 %&& z(i1,j1) ==1
            X(i1,j1)=6;
        elseif P(i1,j1)>0 && Q(i1,j1)<0 && R(i1,j1)<0 && ...
            x(i1,j1)+y(i1,j1)>∆1 %&& z(i1,j1) ==1
            X(i1,j1)=7;
        elseif P(i1,j1)>0 && Q(i1,j1)<0 && R(i1,j1)>0 && ...
            x(i1,j1)+y(i1,j1)>∆1 %&& z(i1,j1) ==1
            X(i1,j1)=8;
        elseif x(i1,j1)+y(i1,j1)≤∆1
            X(i1,j1)=0;
        else
            X(i1,j1)=9;
        end
    end
end

for i2=0:9
    tests(i2+1)=ismember(i2,X);
end

elseif choice=="2"

for i1=1:size
    for j1=1:size
        if P(i1,j1)<0 && Q(i1,j1)>0 && R(i1,j1)<0
            X(i1,j1)=1;
        elseif P(i1,j1)<0 && Q(i1,j1)>0 && R(i1,j1)>0
            X(i1,j1)=2;
        elseif P(i1,j1)<0 && Q(i1,j1)<0 && R(i1,j1)<0
            X(i1,j1)=3;
        elseif P(i1,j1)<0 && Q(i1,j1)<0 && R(i1,j1)>0
            X(i1,j1)=4;
        elseif P(i1,j1)>0 && Q(i1,j1)>0 && R(i1,j1)<0
            X(i1,j1)=5;
        elseif P(i1,j1)≥0 && Q(i1,j1)≥0 && R(i1,j1)≥0
            X(i1,j1)=6;
        elseif P(i1,j1)>0 && Q(i1,j1)<0 && R(i1,j1)<0
            X(i1,j1)=7;
        elseif P(i1,j1)>0 && Q(i1,j1)<0 && R(i1,j1)>0
            X(i1,j1)=8;
        else
            X(i1,j1)=0;
        end
    end
end

for i2=0:8
    tests(i2+1)=ismember(i2,X);
end
```

```
elseif choice=="4"

for i1=1:size
    for j1=1:size
        if P(i1,j1)<0 && Q(i1,j1)>0 && R(i1,j1)<0
            X(i1,j1)=1;
        elseif P(i1,j1)<0 && Q(i1,j1)>0 && R(i1,j1)>0
            X(i1,j1)=2;
        elseif P(i1,j1)<0 && Q(i1,j1)<0 && R(i1,j1)<0
            X(i1,j1)=3;
        elseif P(i1,j1)<0 && Q(i1,j1)<0 && R(i1,j1)>0
            X(i1,j1)=4;
        elseif P(i1,j1)>0 && Q(i1,j1)>0 && R(i1,j1)<0
            X(i1,j1)=5;
        elseif P(i1,j1)≥0 && Q(i1,j1)≥0 && R(i1,j1)≥0
            X(i1,j1)=6;
        elseif P(i1,j1)>0 && Q(i1,j1)<0 && R(i1,j1)<0
            X(i1,j1)=7;
        elseif P(i1,j1)>0 && Q(i1,j1)<0 && R(i1,j1)>0
            X(i1,j1)=8;
        elseif isnan(P(i1,j1))
            X(i1,j1)=0;
        else
            X(i1,j1)=9;
        end
    end
end

for i2=0:9
    tests(i2+1)=ismember(i2,X);
end

end
end
```

7.2.3 Code for Chapter 3.5

The below MATLAB code provides the implicit plot (Figure 3.20) given in Chapter 3.5.

```
∆1=15;
∆2=20;

f = @(a,rho,omega) ∆...
    2*(1+∆2)+((1+∆2)^2*omega-a*rho)*(rho-∆1+omega)/(omega+rho*a/∆2)+(∆2+1)*omega.^2*(
interval = [350 700 12 100 6 40];
fimplicit3(f,interval)
xlabel('a');
ylabel('\rho');
zlabel('\omega');

```

```
xPlane = [700 350 350 700];
yPlane = [12 12 100 100];
zPlane = ∆1-yPlane;
hold on;
patch(xPlane, yPlane, zPlane, 'r', 'FaceAlpha', 0.5);
hold off

xlim([350 700])
ylim([12 100])
zlim([6 40])
```

7.2.4 Code for Chapters 4 and 5

Code used to output figures showing R_i vs. time dynamics as well as 3D plots in Chapters 4 and 5. Nonzero choices of H for Chapter 5 are given by modification of the third equation, shown in comments.

```
%Adapted from Moiseev Igor (2020). Lorenz attaractor plot ...
    (https://www.mathworks.com/matlabcentral/fileexchange/30066-lorenz-attaractor-plo
    MATLAB Central File Exchange. Retrieved June 28, 2020.

clc;
close all;
clear all;

[R1, R2, R3, T] = RBC(1, 1/8, 1/6, 1/120, .3, 24.98, 12.5, 5, ...
    0.21, .166, 6.66, 0, 0, .25, 3, [1.6653 1.249 22.5], 0, 300);
%input (beta, k1, k2, mu3, gamma, s, theta, n, L, alpha, K, mu1, ...
    mu2, A, choice, initV, ts, tf)

% beta - Individual blood regeneration amplifying factor ...
    independent of fractional blood loss
% k1 - Transition rate between R1 and R2 (1/8 in humans)
% k2 - Transition rate between R2 and R3 (1/6 in humans)
% mu3 - Death rate of R3 (1/120 in humans)
% gamma - Individual blood regeneration amplifying factor ...
    dependent on fractional blood loss
% s - Mean steady state value of R3
% theta - Saturation constant for R3 feedback
% n - Sensitivity of feedback with respect to changes in ...
    population size
% L - Constant growth rate of R1
% alpha - Logistic growth rate
% K - Maximum stimulated size of R1 population
% mu1 - Natural apoptosis rate of R1
% mu2 - Natural apoptosis rate of R2
% A - Constant loss from R3
% choice - 1, 2, 3, or 4 for different F and G functions
% initV - Initial value starting conditions
% ts - Time at which to begin simulation
% tf - Time at which to end simulation
```

```
%below are the plots

% figure
% plot3(R1,R2,R3);
% axis equal;
% grid;
% title('Solution Curve (1000 days)');
% xlabel('R_1(x10^{12} cells)'); ylabel('R_2(x10^{12} cells)'); ...
    zlabel('R_3(x10^{12} cells)');

% figure
% ...
    plot3(R1(0.5*length(T):length(T)),R2(0.5*length(T):length(T)),R3(0.5*length(T):le
% axis equal;
% grid;
% xlabel('R_1(x10^{12} cells)'); ylabel('R_2(x10^{12} cells)'); ...
    zlabel('R_3(x10^{12} cells)');
% title('Solution Curve (1000 days) (Long Term Dynamics Only)');

figure
subplot(3,1,1)
plot(T,R1)
title('R_1 vs time');
xlabel('t (days)'); ylabel('R_1(x10^{12} cells)');
subplot(3,1,2)
plot(T,R2)
 title('R_2 vs time');
xlabel('t (days)'); ylabel('R_2(x10^{12} cells)');
subplot(3,1,3)
plot(T,R3)
 title('R_3 vs time');
xlabel('t (days)'); ylabel('R_3(x10^{12} cells)');

% figure
% K = [R1,R2,R3];
% plotmatrix(K)

%end plot section

function [x,y,z,t] = RBC(beta, k1, k2, mu3, gamma, s, theta, n, ...
    L, alpha, K, mu1, mu2, A, choice, initV, ts, tf, T, eps)
if nargin<18 %if too few inputs
  error('MATLAB:lorenz:NotEnoughInputs','Not enough input ...
      arguments.');
end
if nargin<19 %if correct number of inputs
  eps = 0.0000001;
  T = [ts tf];
end
options = odeset('RelTol',eps,'AbsTol',[eps eps eps/10]);
[T,X] = ode45(@(T,X) F(T, X, beta, k1, k2, mu3, gamma, s, theta, ...
```

```
    n, L, alpha, K, mu1, mu2, A, choice), T, initV, options);
x = X(:,1);
y = X(:,2);
z = X(:,3);
t=T;
return
end
function dx = F(T, X, beta, k1, k2, mu3, gamma, s, theta, n, L, ...
    alpha, K, mu1, mu2, A, choice)
%choice determines which of the function choices will be utilized
dx = zeros(3,1);
if choice==1
     dx(1) = beta*(L) - beta*(k1+mu1)*X(1) + ...
         X(1)*gamma*(1/s)*(s-X(3));
elseif choice==2
     dx(1) = beta*(L) - beta*(k1+mu1)*X(1) + ...
         X(1)*gamma*((theta.^n)/(theta.^n + X(3).^n));
elseif choice==3
     dx(1) = beta*alpha*X(1)*(1-X(1)/K) - beta*(k1+mu1)*X(1) + ...
         X(1)*gamma*(1/s)*(s-X(3));
elseif choice==4
     dx(1) = beta*alpha*X(1)*(1-X(1)/K) - beta*(k1+mu1)*X(1) + ...
         X(1)*gamma*((theta.^n)/(theta.^n + X(3).^n));
end
dx(2) = (beta)*(k1*X(1) - (k2+mu2)*X(2));
dx(3) = (beta)*(k2*X(2) - mu3*X(3) );

%dx(3) = (beta)*(k2*X(2) - mu3*X(3) - A*abs(sin(2*pi*T/60-0)));

%dx(3) = (beta)*(k2*X(2) - mu3*X(3) - A);

%%%
% if mod(T,30)<24
%      dx(3) = (beta)*(k2*X(2) - mu3*X(3) );
% else
%      dx(3) = (beta)*(k2*X(2) - mu3*X(3) - A);
% end

return
end
```

Bibliography

[1] W. Boyce and R. DiPrima. *Elementary Differential Equations and Boundary Value Problems*. 10th. Wiley, 2012. ISBN: 9780470458310.

[2] F. Brauer and J. Nohel. *The Qualitative Theory of Ordinary Differential Equations*. 1st. Dover Publications, Inc., 1969. ISBN: 9780486658469.

[3] L. L. Fonseca and E. O. Voit. "Comparison of mathematical frameworks for modeling erythropoiesis in the context of malaria infection". In: *Mathematical Biosciences* 270.Pt. B (2015), pp. 224–236. DOI: `https://doi.org/10.1016/j.mbs.2015.08.020`.

[4] D. H. Fuertinger et al. "A model of erythropoiesis in adults with sufficient iron availability". In: *Journal of Mathematical Biology* 66.6 (2013), pp. 1209–1240. DOI: `https://doi.org/10.1007/s00285-012-0530-0`.

[5] H. Hedrich. *The Laboratory Mouse*. 2nd. Academic Press, 2012. ISBN: 9780123820082.

[6] M. Igor. *Lorenz attaractor plot*. 2011. URL: `https://www.mathworks.com/matlabcentral/fileexchange/30066-lorenz-attaractor-plot` (visited on 01/23/2021).

[7] D. W. Jordan and P. Smith. *Nonlinear Ordinary Differential Equations*. 4th. Oxford University Press, 2007. ISBN: 9780199208241.

[8] K. Kaushansky et al. *Williams Hematology*. ISBN: 9780071833011.

[9] M. C. Mackey. "Unified hypothesis for the origin of aplastic anemia and periodic hematopoiesis". In: *Blood* 51.5 (1978), pp. 941–956. DOI: `https://doi.org/10.1182/blood.V51.5.941.941`.

[10] M. C. Mackey and L. Glass. "Oscillation and chaos in physiological control systems". In: *Science* 197.4300 (1977), pp. 287–289. DOI: `https://doi.org/10.1126/science.267326`.

[11] H. Meijer. *Tutorials on Dynamical Systems software*. 2015. URL: `https://wwwhome.ewi.utwente.nl/~meijerhge/software.html` (visited on 01/23/2021).

[12] C. N. Ngonghala, G. A. Ngwa, and M. I. Teboh-Ewungkem. "Periodic oscillations and backward bifurcation in a model for the dynamics of malaria transmission". In: *Mathematical Biosciences* 240.1 (2012), pp. 45–62. DOI: `http://dx.doi.org/10.1016/j.mbs.2012.06.003`.

[13] G. Ngwa. “On the Population Dynamics of the Malaria Vector”. In: *Bulletin of Mathematical Biology* 68 (2006), pp. 2161–2189. DOI: https://doi.org/10.1007/s11538-006-9104-x.

[14] World Health Organization. *World Malaria Report 2020*. World Health Organization, 2020. ISBN: 9789240015791.

[15] L. Pujo-Menjouet. “Blood Cell Dynamics: Half of a Century of Modelling”. In: *Mathematical Modelling of Natural Phenomena, EDP Sciences* 11 (2016), pp. 92–115. DOI: https://doi.org/10.1051/mmnp/201611106.

[16] G. Sallet and A. H. B. Moacyr. “Monotone dynamical systems and some models of Wolbachia in Aedes Aegypti populations”. In: *Revue Africaine de la Recherche en Informatique et Mathématiques Appliquées* 20 (2015), pp. 145–176. DOI: https://hal.inria.fr/hal-01320616.

[17] M. Tetschke et al. “Mathematical Modeling of RBC Count Dynamics after Blood Loss”. In: *Processes* 6.9 (2018). DOI: https://doi.org/10.3390/pr6090157.

[18] J. J. Thibodeaux. “Modeling erythropoiesis subject to malaria infection”. In: *Mathematical Biosciences* 225.1 (2010), pp. 59–67. DOI: https://doi.org/10.1016/j.mbs.2010.02.001.

[19] W. A. Woldegerima, M. Teboh-Ewungkem, and G. A. Ngwa. “The Impact of Recruitment on the Dynamics of an Immune-Suppressed Within-Human–Host Model of the *Plasmodium falciparum* Parasite”. In: *Bulletin of Mathematical Biology* 81 (2018), pp. 4564–4619. DOI: https://doi.org/10.1007/s11538-018-0436-0.